

See discussions, stats, and author profiles for this publication at: <https://www.researchgate.net/publication/342436184>

Effect of Sunlight/Ultraviolet Exposure on the Corrosion of Fusion-Bonded Epoxy (FBE) Coated Steel Rebars in Concrete

Article in *Corrosion -Houston Tx-* · June 2020

DOI: 10.5006/3588

CITATIONS

5

READS

824

2 authors:



Deepak Kamde

Indian Institute of Technology Madras

22 PUBLICATIONS 32 CITATIONS

[SEE PROFILE](#)



Radhakrishna Pillai

Indian Institute of Technology Madras

145 PUBLICATIONS 742 CITATIONS

[SEE PROFILE](#)

Some of the authors of this publication are also working on these related projects:



Bond performance of pre-tensioned concrete system [View project](#)



PhD work [View project](#)

Effect of Sunlight/Ultraviolet Exposure on the Corrosion of Fusion-Bonded Epoxy (FBE) Coated Steel Rebars in Concrete

Deepak K. Kamde* and Radhakrishna G. Pillai^{†,*}

Currently, highway/railway bridges are designed for the service life of more than 100 y. In such reinforced concrete structures, fusion-bonded epoxy (FBE) coated steel rebars are being used in anticipation of delayed initiation of reinforcement corrosion. However, the FBE steel rebars get exposed to sunlight/ultraviolet rays during prolonged storage and delayed/staged construction. This paper presents micro-analytical and electrochemical data (Fourier transform infrared spectroscopy, scanning electron microscopy, energy dispersion x-ray diffraction, and electrochemical impedance spectroscopy) and shows the adverse effects of sunlight/UV exposure on the corrosion resistance of FBE-coated steel reinforcement in concrete construction. Based on tests on steel-mortar specimens, the mechanisms of UV-induced chemical changes, shrinkage, and cracking of FBE coating, and the resulting steel corrosion mechanisms are proposed. Also, the adverse effects of sunlight/UV exposure on chloride threshold and reduction in the service life of FBE-coated steel in cementitious systems are presented. The paper recommends to minimize the exposure of FBE-coated steel rebars to sunlight/UV rays to less than one month.

KEY WORDS: chloride threshold, concrete, corrosion, epoxy-coating, service life, steel, ultraviolet

INTRODUCTION

Chloride-induced corrosion is one of the major deterioration mechanisms of reinforcing bars (rebars) in concrete structures. Fusion-bonded epoxy (FBE) coated steel rebars are widely used in anticipation of better resistance to chloride penetration and delayed onset of corrosion. FBE coating provides a physical barrier between the underlying steel and surrounding cementitious system—preventing entry of moisture, oxygen, chlorides, etc. Also, FBE coating restricts the ionic flow near the steel surface and limits the formation of anodic and cathodic regions.¹⁻³ FBE-coated steel rebars were introduced in United States in the early 1970s, and later many countries started using them⁴⁻⁵ and banning them as well.⁶⁻⁸

Figure 1 shows the schematic of the cross section of a typical FBE-coated steel rebar embedded in concrete. FBE coating with a thickness of about 175 μm to 300 μm is obtained by placing the steel rebars (maintained at about 230°C) in a mist of powdered epoxy, which is used to fuse and bond to the steel surface.⁶ This fusion bonding and subsequent quenching help to form a uniform, continuous, and well-adhered epoxy coating on the steel surface.⁹ Here, the epoxy coating is expected to insulate the steel surface from the corrosive environment and delay the initiation of corrosion. However, FBE coatings are found to have holidays or pinholes (manufacturing defects). In addition to manufacturing defects, poor handling of FBE-coated steel rebars during transportation and at construction sites lead to scratching and cracking of the epoxy coating, which in turn reduces its corrosion resistance, which is reported many times in the literature.¹⁰ In addition, FBE-coated steels also get exposed to sunlight/ultraviolet (UV)

radiation during prolonged storage and delayed construction, which are difficult to avoid at many construction sites. It was reported that 5 of 300 bridges in Florida, United States faced premature initiation of corrosion due to open storage of FBE-coated steel at construction sites.^{9,11} However, the deterioration mechanism was not discussed. Sagüés, et al., reported that the possible reason for early corrosion in Florida bridges was the combination of the highly aggressive environment (such as heat-cooling cycle, UV exposure), highly permeable concrete, and flaws and damage to FBE coating.¹¹ The scenario could be worse in many parts of the world with poor handling practices and high UV indices. Figure 2 shows that the UV indices in many countries can be more than eight in the month of October. Also, the UV indices can be significantly high during summer, which can be considered as severe exposure conditions for epoxy-coated steel rebars.¹²⁻¹⁴ It should be noted that most of the construction happens during summer. Also, many construction projects experience delays due to several reasons leading to prolonged exposure of the steel rebars to sunlight/UV rays. ASTM A775 suggests that "if circumstances require storing coated steel reinforcing bars outdoors for more than two months, protective storage measures such as steel rebars covered in opaque polyethylene sheeting shall be implemented to protect the material from sunlight, salt spray and weather exposure."¹⁵ Figure 3 shows photographs of FBE-coated steels getting exposed to sunlight/UV during outdoor storage and construction. Also, many agencies in the United States and Europe have banned the use of FBE-coated steel rebars, while many agencies in the rest of the world are still using FBE-coated steel rebars in many projects, and without adequate practices—a serious concern.

Submitted for publication: May 12, 2020. Revised and accepted: June 24, 2020. Preprint available online: June 24, 2020, <https://doi.org/10.5006/3588>.

[†] Corresponding author. E-mail: pillai@iitm.ac.in.

* Department of Civil Engineering, Indian Institute of Technology Madras, Chennai, 600 036, India.

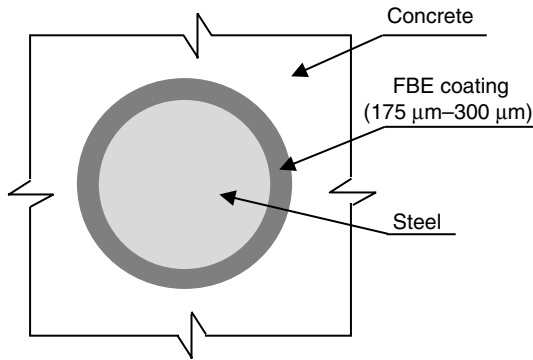


FIGURE 1. Schematic of the cross section of FBE-coated steel rebar embedded in concrete.

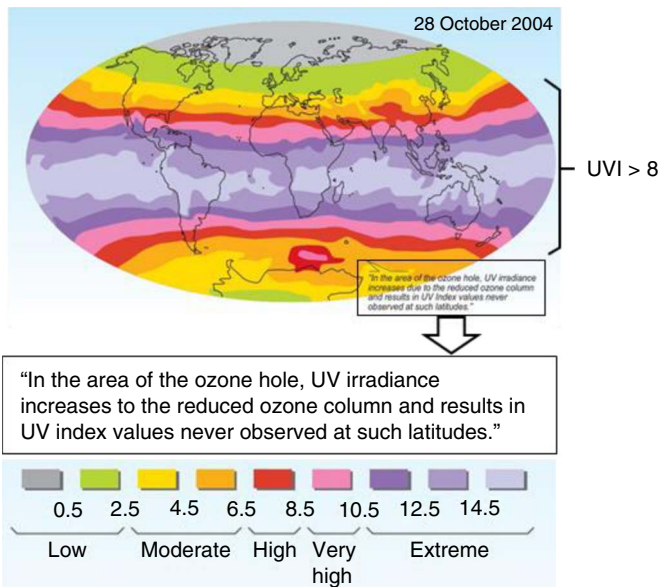


FIGURE 2. Global solar UV index. Republished from UNEP, © 2008.¹³

Literature provides significant information on the propagation of corrosion of FBE-coated steel rebars. However, authors could not find literature on the effects of UV exposure on the “initiation” of corrosion of FBE-coated steel rebars and a corresponding reduction in chloride threshold and

probabilistic service life, which are the focus of this paper. The remainder of the paper presents a review on the performance of FBE-coated metals in various exposure conditions. Then, the effect of exposure to UV rays on the characteristics of FBE coating on steel rebars is evaluated, and the mechanism of the degradation of coating and corrosion initiation is proposed. Following this, the effect of UV exposure on the chloride thresholds and service lives of FBE-coated steel rebars embedded in concrete are estimated. Then, modifications to the recommendations in ASTM A775 (2017) are proposed.

1.1 | Performance Enhancement of Epoxy Coating on Metals

Epoxy resin is a combination of chemical bonds (C-H, C-C, C-O-C, N-H, etc.) formed by the polymerization and crosslinking.¹⁶ The exposure to heat, moisture, and sunlight, can alter the mechanical properties of epoxy resins, which must be considered before using them for a particular engineering application.^{10,17-18} In the case of coatings for steel reinforcement in concrete structures, the desired levels of mechanical properties (i.e., modulus of elasticity, yield strength, and tensile strength) can be achieved by controlled curing and suitable dosage of nanomaterials.¹⁰ For example, barium titanate or barium sulfate is added to control density, achieve high dielectric constant, and tensile strength of epoxy coating.¹⁹ Desired chemical adhesion with steel and resistance to moisture/alkali in concrete can be achieved by the addition of reactive diluents and other additives to epoxy resin.²⁰⁻²¹ Note that the UV-induced changes in the physical and mechanical properties of the epoxy may facilitate oxygen, moisture, and chloride transport to the steel/coating interface.²² This can lead to cathodic disbondment/delamination at the steel/coating interface, which in turn can lead to differential microclimates at various locations in the steel/coating interface. This leads to a change in the chloride threshold of the steel/coating interface and the initiation of corrosion.²³ In general, reactive diluents and other additives are added to epoxy resin to achieve the desired chemical adhesion with steel and resistance to moisture/alkali/UV in coating.²⁰ Typically, such epoxy materials are used for applications on steel rebars.

Total UV irradiance depends on the latitude, altitude above the mean sea level, cloudiness, the time of day, the day of the year, dust in the atmosphere, and on the type and amount of aerosols.²⁴⁻²⁵ At ground level, the sunlight consists of UVA (315 nm to 400 nm) and UVB (280 nm to 315 nm) radiations.¹⁶ The UV radiation can have higher energy than

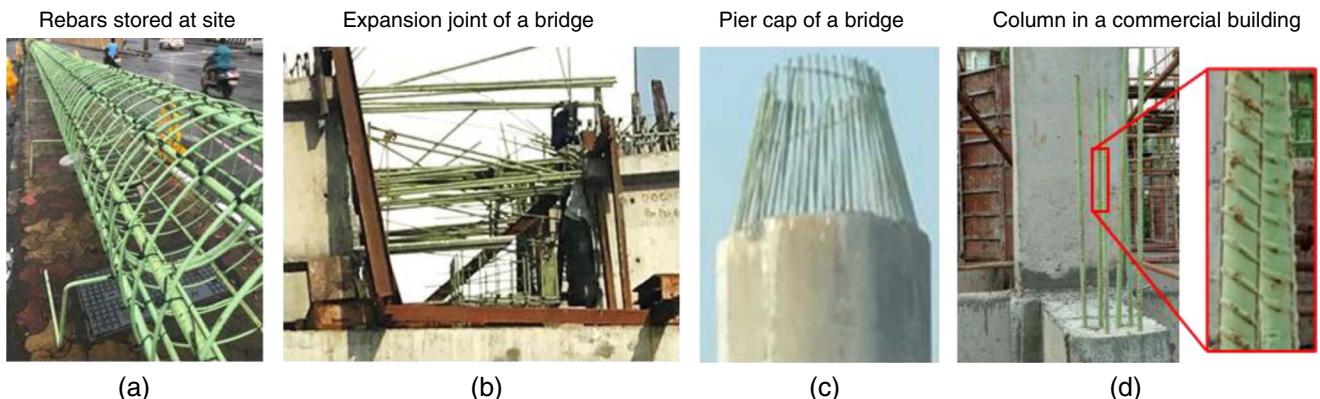


FIGURE 3. Prolonged exposure of FBE-coated rebars (green in color) to sunlight.

-C-H, -N-H, and -O-H bonds in epoxy systems—leading to the breakage of such chemical bonds. The regions with broken chemical bonds can get oxidized and degrade the epoxy coating.¹⁶ To resist the degradation of epoxy coating, the surface of the epoxy can be stabilized by using antioxidants and photostabilizers, such as TiO₂ and ZnO.²⁶ The dosage of stabilizers/additives could alter the performance of the epoxy coating. For example, an increase in the dosage of carbon black nanoparticles (from 0.7 wt% to 2.5 wt% of epoxy resin) could improve the UV resistance by two times (increase from 1,000 h to 2,000 h of resistance to degradation with exposure to UV radiations).²⁷ The particle size of stabilizers can also influence the UV resistance of polymers—the smaller the particle size, the better the UV resistance.²⁸ However, the smaller the particle size, the greater the degree of agglomeration could be, which can be prevented by dispersing small particles in epoxy by electrostatic force or ultrasonic waves.²⁹⁻³⁰ The type of additive also influences UV resistance. For example, UV resistance of inorganic and organic additives depends on the kind and degree of crystallinity and the energy bands of molecular systems. Combinations of inorganic and organic additives have been reported to provide enhanced UV resistance.³¹

The performance of coated steel rebars can be evaluated by the barrier efficiency, coating resistance to electrical or ionic conductivity, and resistance to disbondment of coating.³²⁻³³ It is known that the coatings are permeable to moisture and oxygen.³⁴ Tator reports that the alkaline solution (such as concrete) can break the crosslinking and soften the coating. The disintegration of coating material can lead to a decrease in the ionic or electric resistance of coating.³⁴ In addition, exposure to an alkaline environment (here, cementitious systems), coating defects, etc., can result in increase disbondment of coating.³⁵ The higher the resistance to disbondment of coating, the lower the underfilm/crevice corrosion and its propagation will be. However, the authors could not find literature on the effects of exposure to sunlight/UV rays on the various characteristics of the coating and its disbondment in the case of FBE-coated steel rebars used in concrete construction.

1.2 | Corrosion of Fusion-Bonded Epoxy Coated Steel Rebars and Its Testing

ASTM A775 provides the limits of acceptable defect size for FBE-coated rebars. However, various defects crossing these limits have been observed on numerous FBE-coated steel rebars in use at various construction sites.⁴ In addition,

the poor handling during transportation from factory to the site and the poor handling (bending, cutting, dragging, and stepping/walking over) at construction sites can cause severe damage such as scratches and cracks on the epoxy coating—resulting in premature, localized corrosion.⁵ The use of metallic tie wires and the use of needle vibrators with metallic vibrating heads for compacting the concrete can also lead to severe damage to the FBE-coated steel rebars. In the damaged FBE-coated steel rebars, some of the damaged portions (pinholes or cracks) become the anodes, and the remaining become the cathodes—resulting in localized crevice/underfilm corrosion even without chlorides at the steel rebar level.³ Therefore, practitioners should avoid the use of metallic wires and the use of needle vibrators when using FBE-coated steel rebars. In the 1980s, it was recommended to avoid the bending of FBE-coated steel rebars on site,² which is still in practice in many parts of the world today. Also, the first-generation epoxy coating material was modified with UV-resistant agents and nonbendable epoxy formulations, which exhibited better UV resistance and bonding between the steel and coating and minimizes the progression of underfilm corrosion.²

Table 1 summarizes the literature on concrete structures with FBE-coated steel rebars built with target corrosion-free service lives of about 50 y to 75 y, but showing visible corrosion even within about 5 y.^{8,11} On the other hand, Table 2 shows the summary of laboratory studies indicating mixed opinions (i.e., good and poor performances) on the corrosion resistance of FBE-coated systems. Following are two possible reasons for these differences in opinions between the lab and field studies and between the lab studies: The first probable reason is the use of test methods that are not able to mimic and capture the possible corrosion mechanisms that can occur in FBE-coated systems in the long term (see Table 2). Some literature suggests using the electrochemical impedance spectroscopy (EIS) technique to assess the corrosion performance of coated steel systems,³⁵⁻⁴¹ which is adopted in this study. It should be noted that there are many papers on the corrosion performance of FBE-coated steel rebars reporting the comparative mass loss or cumulative corrosion after periods of exposure to aggressive environments (see Table 2). Also, literature suggests the chloride threshold of FBE-coated steel rebar is 1 wt% to 2 wt% of cement,^{2,42} which is significantly higher than the chloride threshold of uncoated steel rebars (i.e., ≈ 0.4 wt% of cement).⁴³ However, these values are determined based on half-cell potential measurements, macrocell corrosion

Table 1. Field Studies Showing Poor Performance of FBE-Coated Steel Rebars

Location	Age (y)	Conditions/Observations	References
Florida, USA	<20	Outdoor storage; about 5 out of 300 bridges experienced severe corrosion	McDonald ⁹
Minnesota, USA	<35	Cracks and disbondment of coating	
Various states in Canada	5 to 16	Disbondment of coating; underfilm corrosion	Griffith, et al., Pianca, et al. ⁷⁻⁸
Spiez, Switzerland	24	Low chloride level at steel surface; disbondment of coating	Kessler, et al. ⁴⁴
Virginia, USA	5	Disbondment of coating	Pyc, et al. ⁴⁵
Various states (MI, WI, NY, PA, OH, VA, and IA) in USA	<20	Underfilm corrosion, cracking, blistering, and disbondment of coating	Kim, et al., Fanous and Wu, Zemajitis, et al. ⁴⁶⁻⁴⁸
Various bridges in USA	<30	Early corrosion in Florida bridges was the result of combination of highly aggressive environment (such as heat-cooling cycle and UV exposure), highly permeable concrete, and flaws and damage to FBE coating	Sagüés, et al. ¹¹

Table 2. Laboratory Studies and Their Opinion on the Performance of FBE-Coated Steels

Test Method/Technique	Observations	Opinion	References/Country
Salt spray, bendability, long-term exposure of prism specimens to artificial and natural exposure conditions	Good adhesion, toughness, and good resistance to salt water spray and alkaline solution	Good	Swamy, et al. ⁴⁹ /India
Visual observation (VOB), macrocell corrosion (MC)	FBE-coated steel rebars perform good only when they meet the requirements prescribed by ASTM A775	Conditional	Kessler, et al., and Kessler, et al. ^{3,44} /Germany
VOB, half-cell potential (HCP), MC	FBE-coated steel performs well even with damaged coating	Good	Kahhleh, et al., Swamy, et al., and Darwin ^{42,49-50} /USA, India
MC	Irrespective of coating type, coating damage of less than 1% does not have a significant impact on macrocell current behavior	Good	Mohammed, et al. ⁵¹ /India
Linear polarization resistance (LPR)/weight loss	The corrosion rate of undamaged FBE was found to be significantly low. However, corrosion rate increased with the increase in damage area	Good	Al-Amoudi, et al. ⁵² /Saudi Arabia
VOB, HCP, MC	FBE-coated rebars were intact even after exposure to chloride solution for about 8.5 y	Good	Scannell and Clear ⁵³ /USA
VOB and electrochemical impedance spectroscopy (EIS)	No evidence of corrosion even with cracked concrete; resistance of high-frequency loop was low with damaged coating	Good	Lau and Sagüés ³⁹ /USA
HCP, EIS	Measurement of HCP can be misleading; there was delamination of the coating after 1 y exposure to 3.5% NaCl solution. However, the corrosion rate was low	Good	Darwin and Scantlebury ⁵⁴ /UK
VOB, HCP, MC, EIS	Review paper	Mixed opinion	Zemajitis, et al. ⁴⁸ /USA
Coating adhesion, HCP, MC	No correlation with the rate of corrosion and measured corrosion potential	Mixed	Cortés ² /USA
LPR, EIS	Underfilm corrosion	Poor	Singh and Ghosh ⁵ /Saudi Arabia

current, and linear polarization resistance (LPR), which may not be valid for reinforced concrete systems with FBE-coated steel rebars. Also, literature shows that the chloride thresholds of damaged FBE-coated steel rebars are 1 to 5 Cl⁻/OH.³ In particular, the authors could not find literature on chloride threshold at the steel/coating interface, which is needed to estimate service life. The second reason for differences in opinion between lab/field studies is the possible difference between the quality of FBE-coated steel rebars tested in the laboratories and that used in construction sites. At sites, by the time the FBE-coated steel rebars are placed in concrete, they could experience significant damage and get exposed to sunlight/UV rays during storage and delays in construction stages (see Figure 3). Moreover, authors could not find literature on the degradation of FBE-coated steel rebars due to the exposure to sunlight/UV rays and its effects on the initiation of corrosion and reduction in the service life of concrete systems, which is the focus of this paper.

RESEARCH SIGNIFICANCE

Based on field and laboratory studies, many agencies in the United States, Canada, and Europe have stopped using FBE-coated steel rebars in concrete construction. However, India, China, Japan, Germany, and some parts of the United States are still using them—a few of these are able to strictly enforce stringent quality control measures on materials and construction practices, while many are not able to; the latter case is a huge concern. Moreover, due to prolonged outdoor

storage and delays in construction, FBE-coated steel rebars get exposed to sunlight/UV radiations, the effects of which on corrosion resistance are not well reported in literature. This paper provides an experimental database and the evidence on adverse effects due to sunlight/UV exposure and sensitizes the engineers to ensure shaded storage of FBE-coated steels and minimize delays in construction. This paper reveals that, at a place with high UV index, exposure to sunlight for about 1 month could crack the epoxy coating, leading to a significant reduction in its resistance to chloride attack, chloride-induced corrosion, and service life.

EXPERIMENTAL METHODS

The experiments were conducted in two phases. Phase 1 involved studies on the effect of UV exposure on the degradation of epoxy coating. Phase 2 involved studies on detecting corrosion initiation using EIS techniques and quantification of the effect of UV radiation on chloride threshold (Cl_{th}), which is defined as the amount of chlorides at the steel surface (i.e., at steel/cementitious interface in the case of uncoated steels and at the steel/coating interface in case of coated steels) required to initiate active corrosion.

3.1 | Phase 1: Exposure to Ultraviolet Rays and Coating Characteristics

Typical daylight (wavelength of 300 nm to 340 nm) can be simulated using UVA tube lamps (340 nm), which can be used for

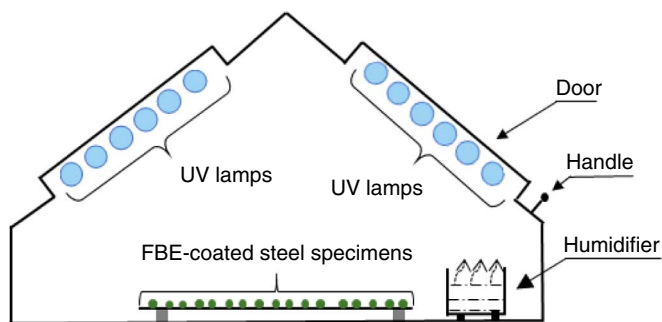


FIGURE 4. The UV chamber used for artificial weathering of FBE-coated rebars.

accelerated screening tests.⁵⁵ For this, a UV chamber (1.5 m × 0.5 m × 0.5 m) with 12 UVA tube lamps and a humidifier was fabricated, see Figure 4.⁵⁶ Cyclic UV exposure (8 h with UV lights “ON” followed by 4 h of the humid environment with UV lights “OFF”) was maintained using a timer. For this, the chamber was sealed, and the humidifier was run for 15 min at the beginning of the humid period. A total of 45 as-received FBE-coated steel rebars with “no damage or degradation” (denoted as FBEC-ND; each with 8 mm diameter and 50 mm length) were kept in UV chamber for 60 d. Table 3 shows the test variables and the number of specimens cast for Phase 1 of this study. Here, “no damage” indicates that no intentional damage was made on the specimens. The UV radiation was maintained to be uniform over the length of the tube lamps (as per ASTM G154). The three specimens each were removed after 0, 1, 3, 7, 10, 12, 15, 20, 25, 30, 35, 40, 45, 55, and 60 d of exposure. Then, the specimens were stored in a dark container until tested for changes in coating characteristics. A 5 mm × 5 mm size sample of the coating was peeled-off from the exposed surface (i.e., top surface) of each rebar specimen. Micrographs of these samples were obtained using the scanning electron microscope (SEM) and the initiation and widening of cracks as a function of the

duration of UV exposure were studied. The chemical composition and atomic bond characteristics of three coating samples (with 0 and 10 d of UV exposure) were obtained from three coating samples of each type using energy dispersion x-ray (EDX) and Fourier transform infrared (FTIR) spectra. Literature report that the epoxy-based coatings can crack between 10 d and 15 d of artificial weathering.^{16,57} Similar results are observed in the current study using the artificial weathering test method prescribed in ASTM G154 (2016). Also, to obtain the relation between damage due to exposure to artificial and natural weathering, FBE-coated rebars were exposed to natural sunlight for about 1.5 months in summer in Chennai (24°C to 39°C; 37% to 78% RH, and UV index of ≈10).⁵⁸ With this test data and the literature,⁵⁹ it was found that the abovementioned artificial weathering of about 10 d is equivalent to about 1 month of natural exposure to sunlight.

3.2 | Phase 2: Corrosion Initiation, Chloride Threshold, and Service Life

3.2.1 | Preparation of Lollipop Type Test Specimen

In this study, the chloride threshold is defined as the chloride concentration at the steel surface (i.e., at the steel/mortar interface for uncoated rebars and at the steel/coating interface for FBE-coated rebars) that is required to initiate active corrosion. Figure 5 provides a photograph and schematic of the lollipop test specimen with a steel reinforcement embedded at the center of a mortar cylinder.⁶⁰ Five lollipop test specimens each were cast with the following types of steels: (i) uncoated, (ii) FBE-coated steel in as-received condition with “no damage or degradation” (FBEC-ND), and (iii) FBE-coated steel with 10 d of UV exposure (FBEC-UV). Table 3 shows the test variables and the number of specimens cast for Phase 2 of this study. For this, 5 uncoated and 10 FBE-coated steel rebars of 8 mm diameter and 110 mm long were cut. Then, five FBE-coated steel rebars each were placed in the UV chamber for 0 and 10 d, respectively (i.e., for casting five FBEC-ND and five FBEC-UV specimens). Later, a 3.4 mm diameter hole was drilled at one end of the steel. This drilled hole was threaded

Table 3. Test Variables and Number of Specimens Used for Phase 1 and Phase 2

Phase	Coating Condition	Properties	Type of Specimens	Number of Specimens
Phase 1	FBEC-ND	Coating integrity and chemical composition	5 mm × 5 mm coating samples peeled off from rebars	3
		Atomic bonding		3
	FBEC-UV	Coating integrity and chemical composition	5 mm × 5 mm coating samples peeled off from rebars exposed to UV rays	42
		Atomic bonding		3
Phase 2	Uncoated	Chloride threshold	Lollipop specimens	5
	FBEC-ND	Resistance of coating		5
		Chloride thresholds	Coating specimens (extracted from the steel in lollipop specimen after exposure test)	15
		Chloride diffusion coefficients		15
	FBEC-UV	Resistance of coating	Lollipop specimen	5
		Chloride thresholds	Coating specimen (extracted from the steel in lollipop specimen after exposure test)	10
Chloride diffusion coefficients		10		

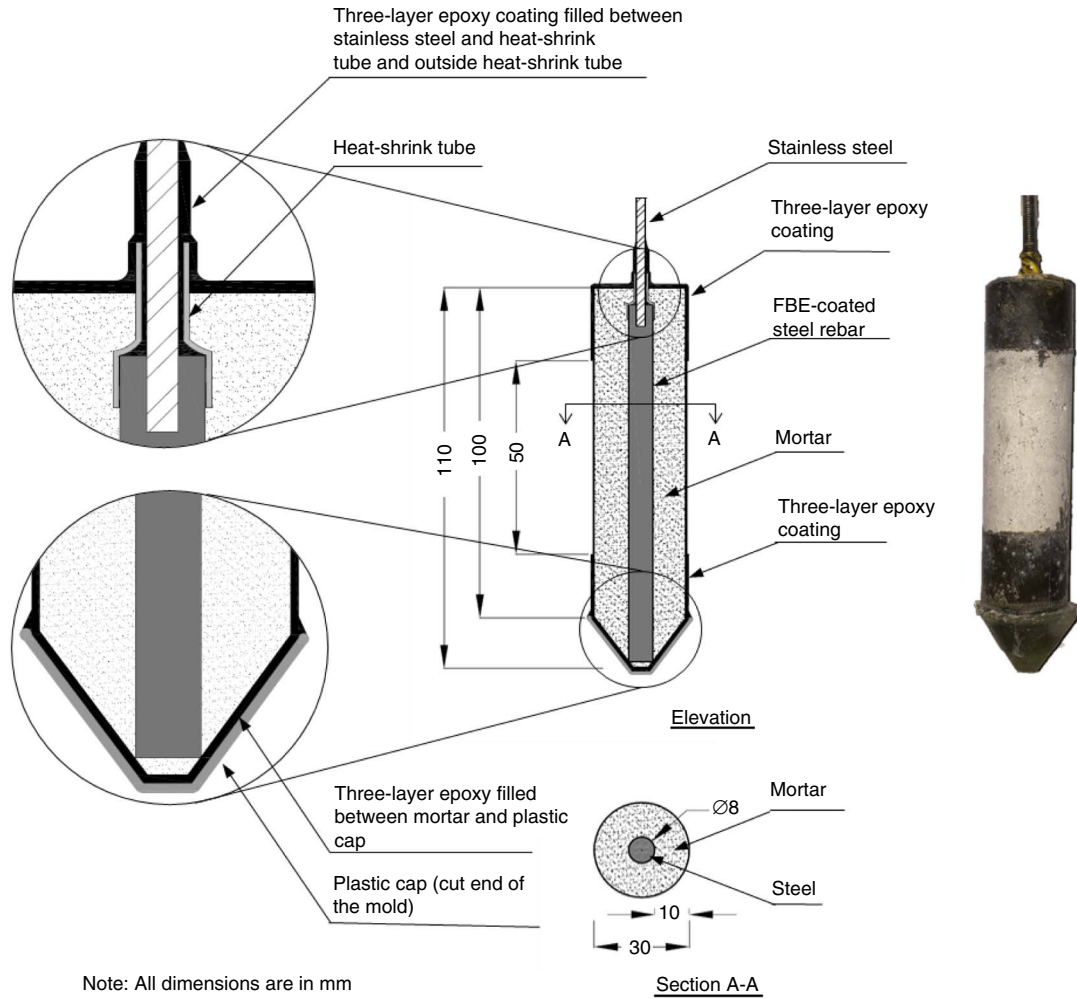


FIGURE 5. Lollipop specimen used for electrochemical testing.

and a stainless steel threaded rod was fastened to make electrical connections for electrochemical tests. The uncoated steel pieces were cleaned and degreased using ethanol and ultrasonic cleaner. Thereafter, the 5 mm long portion at the end of steel rebar (including the junction of steel rebar and stainless steel rod) was covered with two thin layers of epoxy and cured as per manufacturers' recommendations. It was ensured that the epoxy was resistant against the highly alkaline mortar for the duration of testing and had electrically insulated the steel from the adjacent mortar. Later, after curing, this portion and 10 mm of stainless steel threaded rod was covered with a heat shrink tube. The gap between heat shrink tube and stainless steel was filled with low viscosity epoxy to avoid entry of moisture or chloride during the exposure and testing (see the close-up image in Figure 5). The prepared steel pieces were placed in plastic cylindrical molds (110 mm long and 30 mm inner diameter) with a conical bottom to facilitate the positioning of the rebar at the center of the cylinder. Mortar with water:binder:sand ratio of 0.5:1:2.75 was placed in molds to achieve a cover depth of about 10±1 mm. The specimens were cured in plastic molds for 1 d in the laboratory environment (25±2°C and 65±5% relative humidity). Then, they were removed from plastic molds and moved to a fog room (25±2°C and 95±5% relative humidity) for 27 d. After curing, the specimens were moved to the laboratory at

25±2°C and 65±5% relative humidity and allowed to dry for 48±4 h. Then, the mortar surface, except the 50 mm long portion at the center, was coated with two layers of epoxy (see Figure 5). Each layer of epoxy was allowed to cure for 24 h each. This ensured that the chloride ingress would happen only through the 50 mm long uncoated portion at the center. This could also avoid preferential underfilm corrosion of the epoxy-coated end regions of rebars, which was verified after autopsying the specimens at the end of corrosion testing.

3.2.2 | Corrosion Cell, Cyclic Exposure, and Repeated Electrochemical Impedance Spectroscopy Tests

Figure 6 shows the schematic of the corrosion cell used for cyclic chloride exposure and repeated EIS tests. The cyclic wet-dry exposure consisted of 2 d of wetting with 3.5% NaCl solution followed by 5 d of natural drying in the laboratory. Here, the embedded steel rebar is the working electrode, the nickel-chromium mesh placed circumferentially to the lollipop specimen is the counter electrode, and a saturated calomel electrode (SCE) is the reference electrode. The chloride-contaminated simulated concrete pore solution (SPS) ([0.03% Ca(OH)₂ + 2.32% KOH + 1.04% NaOH + 3.5% NaCl + 96.6% distilled water] of wt% of solution) was used as the

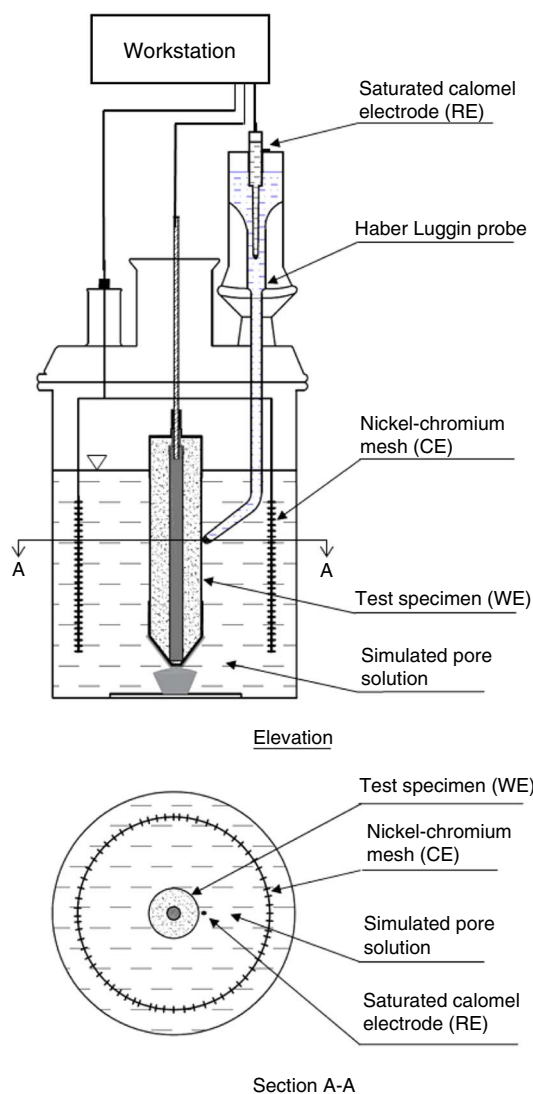


FIGURE 6. Three-electrode corrosion cell.

immersion solution. The EIS response was obtained at the end of each wet period by using the procedures and input variables suggested by Rengaraju, et al.⁶⁰ An AC potential amplitude of ± 10 mV and a frequency range of 1 MHz to 0.01 Hz were used. Also, the DC potential was maintained at OCP and 10 data points per decades were collected.

Figure 7 shows the ideal EIS response (Nyquist plot) that could be from FBE-coated steel with no damage and degradation embedded in cementitious systems and the equivalent electrical circuit (EEC).^{39,41,61-62} As shown, the response can have three pure loops, corresponding to mortar, FBE coating, and steel/coating interface (S-C), respectively. The response was analyzed, and resistance offered by each layer (coating and steel/coating interface) was quantified using the equivalent electrical circuit shown in Figure 7. CPE_C and R_C are the capacitance and resistance of the coating, respectively. Depending on the quality of FBE coating, its resistance may reduce as the testing involves continued exposure of the coating to moisture/alkaline environment for many weeks. If its resistance remains high for a long duration, then the ingress of moisture, chloride, and oxygen through the coating will take a

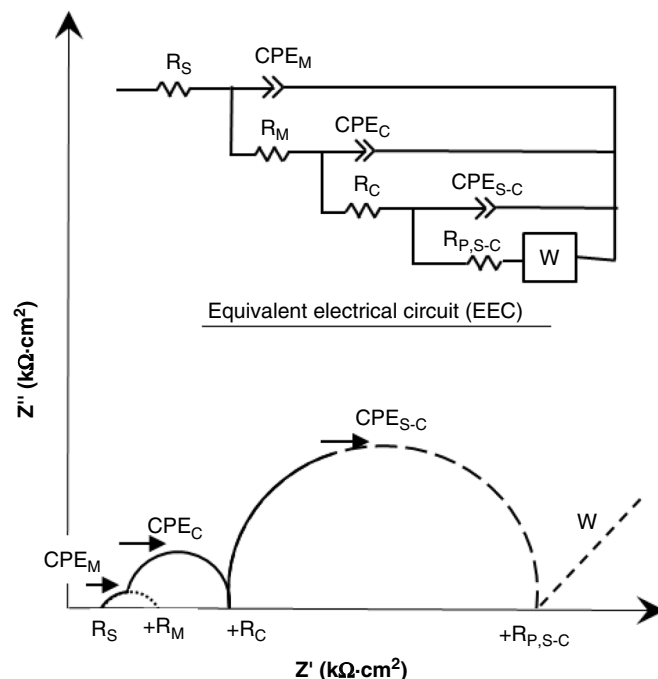


FIGURE 7. Ideal Nyquist plot and EEC for FBE-coated steel in mortar.

long time to reach the steel surface. In this study, R_C was monitored throughout the testing to assess the degradation process of FBE coating. The CPE_{S-C} and $R_{P,S-C}$ are the capacitance and resistance to polarization of the steel/coating interface, respectively. To detect the initiation of corrosion, $R_{P,S-C}$ was monitored during the testing. When five consecutive values of inverse polarization resistance (i.e., $1/R_{P,S-C}$) lie within a boundary of $(\mu \pm 1.3\sigma)$, the system was considered to be in a "stable state" (μ and σ are mean and standard deviation of $1/R_{P,S-C}$). Following this "stable state," if two future measurements lie above $(\mu + 3\sigma)$, then active corrosion was defined to be initiated.^{60,63} Note that the electrical parameters of the solution and mortar (resistance of solution [R_S], the capacitance of mortar [CPE_M], and the resistance of mortar [R_M]) were not monitored as they are out of the scope of this paper.

3.2.3 | Determination of Chloride Threshold of Steel

Upon initiation of active corrosion, the specimens were autopsied, and then about 0.5 mm thick mortar adjacent to the coated steel surface was scraped using a coarse file, collected, and powdered. The chloride concentration in the powder was determined using the guidelines prescribed in SHRP-S-330 (1993).⁶⁴ This was defined as the chloride threshold of the uncoated specimens. However, this is not the chloride threshold for the FBE-coated specimens because these chlorides do not take part in the corrosion process, as the FBE coating separates it. The chloride concentration beneath the coating (i.e., at the steel/coating interface) takes part in the corrosion process; hence, it is considered as the chloride threshold of the FBE-coated steel rebars.⁶⁵ To determine the chloride concentration at S-C interface, EDX analysis was done along the fractured surface of FBE coating.³³ To avoid cross-contamination of chlorides at various depths of thin epoxy coating, the coatings for chloride measurements were not cut using a mechanical tool. Instead, the coated steel rebars were cut

to half of the cross section. Then, the remaining half of the rebar (including coating) was bent and fractured along the cutting plane. The chloride concentration in the coating, close to the steel/coating interface was determined using EDX analysis and defined as the $C_{l_{th}}$ of FBE-coated steel. During EDX tests, an electron beam with energy 20 keV and working distance was maintained to ≈ 10 mm. Note that the measured concentrations are in percentage of chloride by weight of substrate (coating with pores), which represents the local chloride concentration at the location of testing. Therefore, the average of measurements from three locations at the S-C interface was considered (in wt% of FBE coating). To convert this to wt% of binder (%bwob), the chloride concentrations in the mortar adjacent to the coating surface (determined as per SHRP-S-330⁶⁴) were considered equal to the chloride concentration in the coating adjacent to the mortar surface (determined using EDX analysis). Similarly, the relative chloride concentrations at the steel/coating interface were determined (in %bwob) from five specimens of each type and were defined as the $C_{l_{th}}$ of FBE-coated steel rebars.

3.2.4 | Determination of Chloride Diffusion Coefficient of Coating and Service Life

The coating samples were fractured as it was done for determining chloride threshold (see Section 3.2.3, *Determination of Chloride Threshold of Steel*) and then, the chloride profiles were obtained along the cross section (thickness) of the fractured surface of FBE coating. These chloride profiles were used to determine the chloride diffusion coefficients of coating ($D_{cl,coating}$) for FBEC-ND and FBEC-UV coatings. Using the maximum chloride concentrations at the surface of concrete, D_{cl} of concrete, maturity constant (m), concrete cover thickness (x), $C_{l_{th}}$ of steel, and the $D_{cl,coating}$, the service lives of reinforced concrete systems were estimated. For this, the MATLAB[†] program based on Ficks' second law of chloride diffusion through concrete published by Rengaraju⁴³ was modified to accommodate the effect of diffusion of chlorides through the thin epoxy coating (see Equations [1] and [2]). For this, chlorides at concrete surface (C_S) were assumed to diffuse through concrete and reach the coating/mortar interface as per Ficks' second law of diffusion (see Equation [1]).

$$C(x,t) = C_S - (C_S - C_i) \times \operatorname{erf}\left(\frac{x}{\sqrt{(4 \times D_{cl,concrete} \times t)}}\right) \quad (1)$$

where $C(x, t)$ is the chloride concentration measured at depth x from the exposed concrete surface at the exposure time of t seconds; C_S is the surface chloride concentration built-up on the exposed concrete surface after exposure time of t seconds; C_i is the initial chloride concentration in concrete, which is assumed to be zero in this study; $D_{cl,concrete}$ is apparent chloride diffusion coefficient; and $\operatorname{erf}()$ is the mathematical error function. Here, $D_{cl,concrete}$ is considered as a time-variant function. Then, for each interval, the chlorides at the coating/mortar interface were considered as the surface chloride concentration of the coating. Then, using the experimentally determined chloride diffusion coefficient of coating and Ficks' law (Equation [2]), the concentration of chloride at the steel/coating interface was determined. When the concentration of chloride was equal to or more than the chloride threshold of the steel/coating interface (reported in this paper), it was defined as the corrosion-

free service life (i.e., time taken to initiate corrosion) of reinforced concrete. Further details are provided in Kamde.⁶¹

$$C(x_{epoxy},t) = C_{C-M} - (C_{C-M} - C_{i,coating}) \times \operatorname{erf}\left(\frac{x_{epoxy}}{\sqrt{(4 \times D_{cl,coating} \times t)}}\right) \quad (2)$$

where $C(x_{epoxy}, t)$ is the chloride concentration at the depth x_{epoxy} at the time t in the epoxy coating. x_{epoxy} is the depth in the epoxy coating from the coating/mortar interface, C_{C-M} is the chloride concentration at the coating/mortar interface, $C_{i,coating}$ is the initial chloride concentration in the FBE coating, and $D_{cl,coating}$ is the chloride diffusion coefficient of FBE coating, which is determined this study and assumed to be constant throughout the life of the reinforced concrete systems.

RESULTS AND DISCUSSION

4.1 | Phase 1: Exposure to UV Rays and Coating Characteristics

Table 4 provides the chemical composition at the surface of epoxy coating extracted/peeled off from three locations on the FBEC-ND and FBEC-UV samples using EDX. It shows that the concentrations of Ti and Zn on the three FBEC-ND specimens varied significantly, which can be attributed to the variation in the concentration of photostabilizers (i.e., TiO_2 and ZnO) on the surface of epoxy coating—possibly a manufacturing defect. Also, it was found that the concentrations of TiO_2 and ZnO were negligible at cracks on the surface of FBEC-UV samples—indicating that with the deficiency of TiO_2 and ZnO, the epoxy coating can get degraded and microcracks can form within 10 d of laboratory exposure to UV (340 nm) rays (see Table 4). The regions with depletion of photostabilizers such as TiO_2 and ZnO can also undergo photodegradation.²⁷ On the other hand, barium and sulfur were found in the bulk of epoxy coating—indicating that barium sulfate ($BaSO_4$) was added to the epoxy material—probably to enhance the bond between steel and epoxy coating.¹⁹ However, the addition of barium sulfate can increase the brittleness, which in turn can lead to cracking of coating when the bar is bent and the epoxy coating at the outer surface of the bent gets elongated.⁶⁶ The chemical composition of FBEC-ND and FBEC-UV specimens is presented in Table 4. In the case of UV specimens, the composition at and away from cracks are presented.

Figures 8(a) through (l) show the SEM micrographs obtained from the surface of epoxy coating samples at 0, 10, 12, 15, 20, 25, 35, 40, 50, 55, and 60 d of cyclic exposure to artificial weathering in UV chamber. Figure 8(a) is from a FBEC-ND specimen and Figures 8(b) through (l) are from FBEC-UV specimens with specific days of exposure, as mentioned in the images. The photostabilizers (i.e., TiO_2 and ZnO) could prevent disintegration/microcracking of the coating until 10 d of UV exposure in the laboratory. Figure 9 summarizes the crack widths shown in these SEM micrographs and shows the increase in crack width as a function of the duration of UV exposure. As per Figures 8(a) through (l) and Figure 9, the microcracking initiated at about 10 d of exposure to UV radiation in the laboratory. This cracking can be due to the deficiency of photostabilizers on the surface of the epoxy coating, which in turn exposes the bulk material and allows its disintegration. The crack width was increasing up to 25 d of exposure to UV radiation. Then, the crack width was stabilized for the next about 25 d of exposure; this could be due to the presence of

[†] Trade name.

Table 4. Chemical Composition of FBE Coating Specimens^(A)

Element	FBEC-ND		FBEC-UV				$\mu 2 - \mu 3$
			Away From Cracks		At Crack		
	$\mu 1$	CoV	$\mu 2$	CoV	$\mu 3$	CoV	
C	54.4	0.2	50.3	0.3	52.2	0.3	-1.9
N	2.4	1.7	0.5	1.4	3.1	1.2	-2.6
O	13.3	5.6	11.2	0.4	14.3	0.2	-3.1
Mg	1.5	0.5	0.5	1.6	0.4	1.5	0.1
Si	3.3	0.7	3.1	0.5	2.0	0.7	1.1
Ca	3.7	0.94	2.8	0.8	1.7	1.5	1.1
S	22.4	1.0	13.1	1.6	20.5	0.5	-7.4
Ba	12.13	1.8	1.5	1.2	14.0	0.5	-12.5
Ti	4.65	1.7	8.6	1.2	0.3	1.5	8.3
Zn	0.9	1.1	2.0	0.5	0.3	1.2	1.7

^(A) μ : Mean, CoV: Coefficient of variation.

photostabilizers in the bulk coating, which is relatively better protected by the outer layers of coating (i.e., typical sigmoid curve as seen in shrinkage behavior of materials). The evidence of this shrinkage-induced cracking is discussed later in this section. With further exposure, the crack width was found to increase rapidly at about 50 d in the UV chamber (i.e., from about 0.5 mm to 1 mm)—indicating the rupturing of the coating.

The coating started to crack after 10 d in UV chamber (see Figure 8(c)), which is equivalent to about 1.5 months of exposure to sunlight. To validate this, Figure 10 shows the micrographs of coating in three cases: (a) without exposure to UV radiation, (b) with 10 d of exposure to UV radiations in the laboratory, and (c) with 45 d of exposure to natural environment/sunlight at Chennai, India with UVI > 8. The latter two cases resulted in significant long and wide cracks. Therefore, 10 d of exposure in UV chamber is considered for studies in Phase 2.

To investigate the reason for cracking, FTIR spectra (for the range of 600 cm^{-1} to $4,000\text{ cm}^{-1}$) were obtained from epoxy coating samples subjected to 0 and 10 d of UV exposure in the laboratory (see Figure 11). The first, second, third, and fourth regions shown in the spectra range from 600 to $1,500\text{ cm}^{-1}$, $1,500$ to $2,000\text{ cm}^{-1}$, $2,000$ to $2,500\text{ cm}^{-1}$, and $2,500$ to $4,000\text{ cm}^{-1}$, respectively. The first region contains characteristic peaks for the individual bonds such as -C-O and -C-H in epoxy coating.⁶⁷ After exposure to UV rays, the intensity of peaks between $1,000$ and $1,200\text{ cm}^{-1}$, and at $2,932\text{ cm}^{-1}$ decreased—indicating the breakage of -C-H bonds.⁶⁸⁻⁶⁹ In addition, the peaks at $1,231\text{ cm}^{-1}$, $1,296\text{ cm}^{-1}$, and $1,463\text{ cm}^{-1}$ disappeared after exposure to UV rays—indicating the breakage of bonds in CH_2 . In the case of FBEC-ND samples, peaks were observed at 860 cm^{-1} and 970 cm^{-1} —indicating the presence of benzene. When exposed to UV rays, an additional peak was observed at $1,508\text{ cm}^{-1}$ —indicating that the benzene did not undergo photodegradation until 10 d of UV exposure in the laboratory—in agreement with literature.⁶⁹ The FTIR spectra obtained from the FBEC-ND and FBEC-UV samples show that the hydroxyl groups are the weakest bonds in the epoxy coating used in this study. The available sites after the breakage of hydroxyl bonds can get oxidized. The decrease in the area under the curve between $1,550\text{ cm}^{-1}$ and $1,750\text{ cm}^{-1}$ (between

the two vertical dashed lines in Figure 11) indicates the formation of the carbonyl group. The formation of the carbonyl group is a result of the photodegradation process of epoxy polymer, which can result in shrinkage-induced cracking of coatings.^{16,70} This observation on carbonyl group formation justifies the shrinkage-induced cracking phenomenon proposed earlier in this section (i.e., the sigmoid curve until about 50 d followed by a rapid increase in crack width), discussed in Figure 9.

Figure 12 shows the Nyquist plots of the FBEC-ND and FBEC-UV specimens. Note that the time constant for mortar is not shown because the resistance offered by mortar is the same in both cases (i.e., FBEC-ND and FBEC-UV), and is significantly less than the resistance of either coating or steel/coating interface. Also, the electrical parameters of the mortar were not monitored because it is out of the scope of this paper. The resistance of coating (R_c) from FBEC-UV specimens with significant cracking exhibited a resistance of $\approx 5\text{ k}\Omega\text{cm}^2$, which was significantly less than that of FBEC-ND specimens (i.e., $\approx 30\text{ k}\Omega\text{cm}^2$). This indicates that the type of cracks formed in such coatings can provide easy pathways for deleterious elements such as moisture, oxygen, chlorides, etc. to reach the steel surface. Therefore, the authors suggest that FBE-coated steel rebars should not be exposed to sunlight for more than 1 month (including storage and construction stages).

4.2 | Phase 2: Chloride-Induced Corrosion and Service Life

4.2.1 | FBEC-ND: Coating Degradation and Corrosion Initiation

Figure 13 shows the degradation of FBEC-ND and FBEC-UV systems in terms of the change in coating resistance, R_c . Figure 13(a) shows the four-stage degradation process of FBEC-ND coating in cement mortar (alkaline in nature). The first five plots indicate the data from five specimens and the last drawing shows the proposed five-stage degradation process for FBEC-ND systems. Stage 1 is defined as the period when the resistance of coating (R_c) embedded in mortar is constant (say, during the first few weeks of exposure)—indicating that

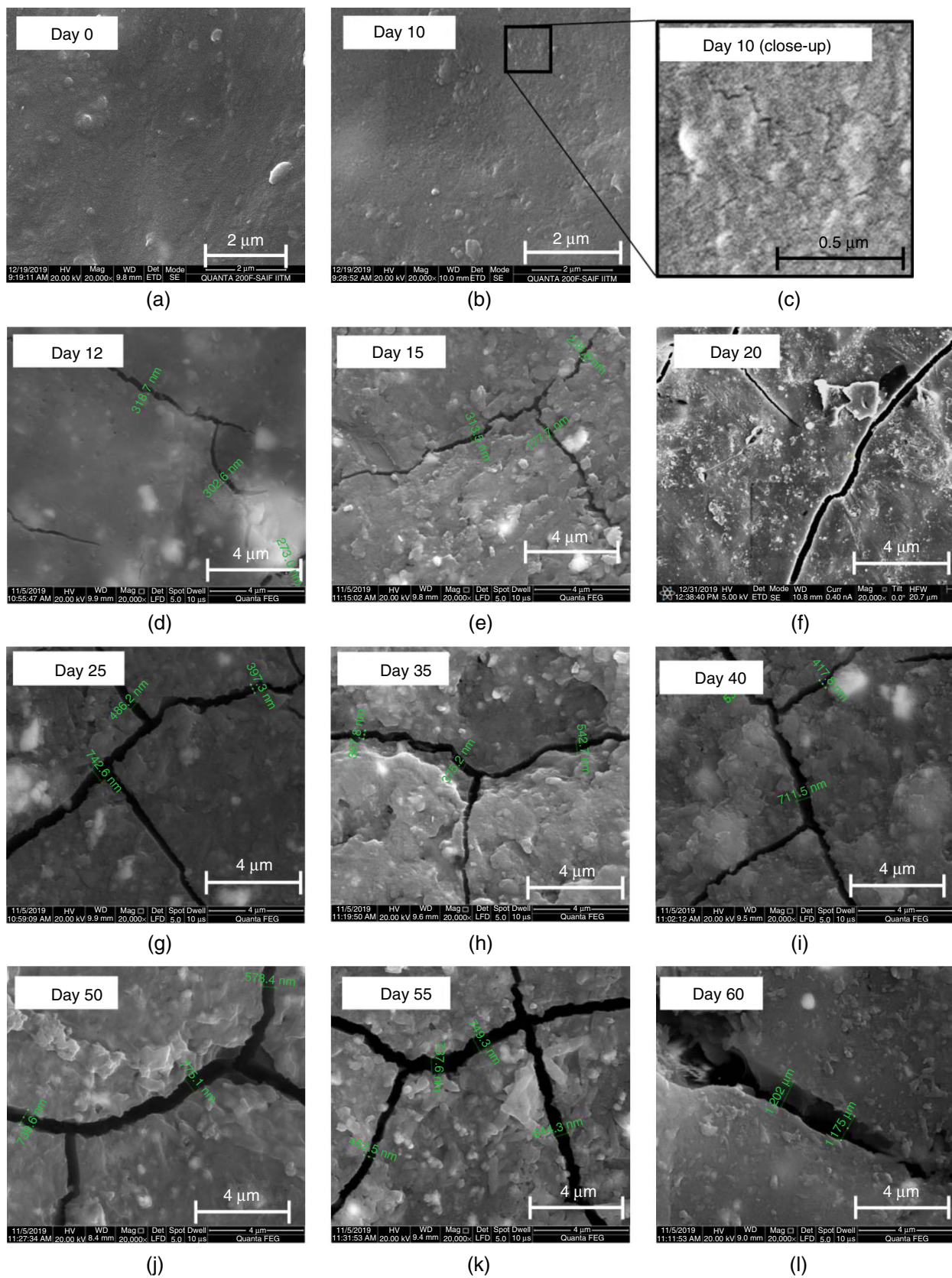


FIGURE 8. Micrographs obtained from (a) FBEC-ND, and (b) through (l) FBEC-UV coating showing crack evolution on epoxy coatings.

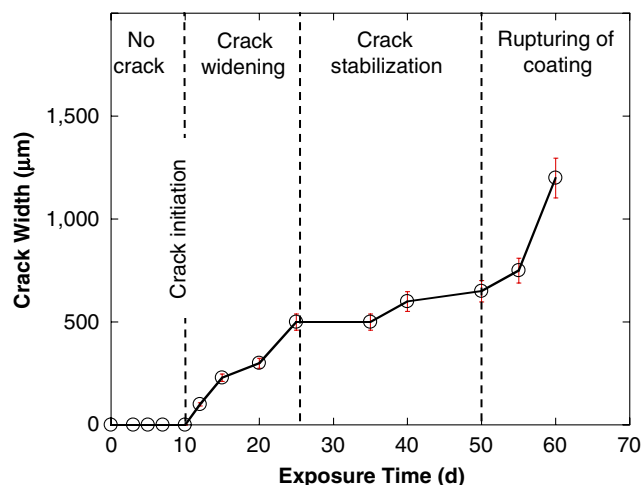


FIGURE 9. Effect of UV exposure on crack width on FBE coating surface.

the coating could resist the entry of alkaline pore solution and moisture for about 3 to 4 weeks. Stage 2 is defined as the period when the R_C decreases. Typically, R_C decreases to about half the original value after first wet period. Similar responses were also reported by Zayed and Sagüés.⁷¹ During this time, the alkaline pore solution and moisture (probably chlorides as well) could have partially penetrated the undamaged coating and reduced the R_C . Then, when sufficient moisture and oxygen are available at the steel surface, corrosion might initiate and propagate. Stage 3 is defined as the period when R_C increases, which can be attributed to the additional resistance offered by pores in the inner layer of coating (i.e., near the steel surface) that are densely filled with corrosion products.³³ This filling of pores at the inner layer of epoxy coating with corrosion products was confirmed by microanalytical analysis (SEM and EDX analysis) of the pores. This can obstruct the further entry of oxygen and delay the corrosion process. In Stage 4, the corrosion products continue to build up, resulting in increased expansive stresses and cracking of coating, which in turn increases the interconnectivity of pores/holidays/cracks and

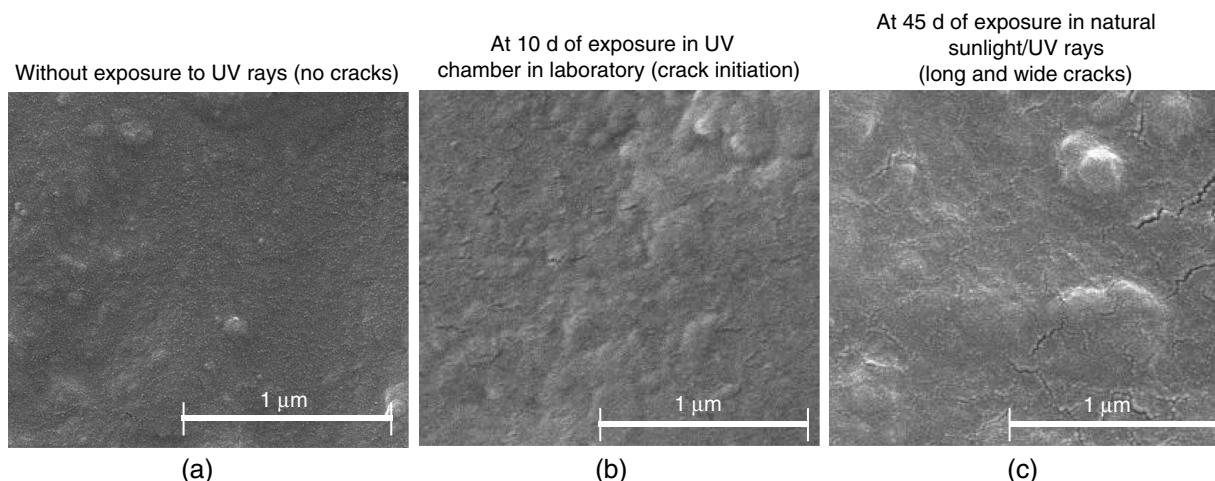


FIGURE 10. Cracks on FBE coatings formed due to exposure to UV rays in artificial weathering versus sunlight.

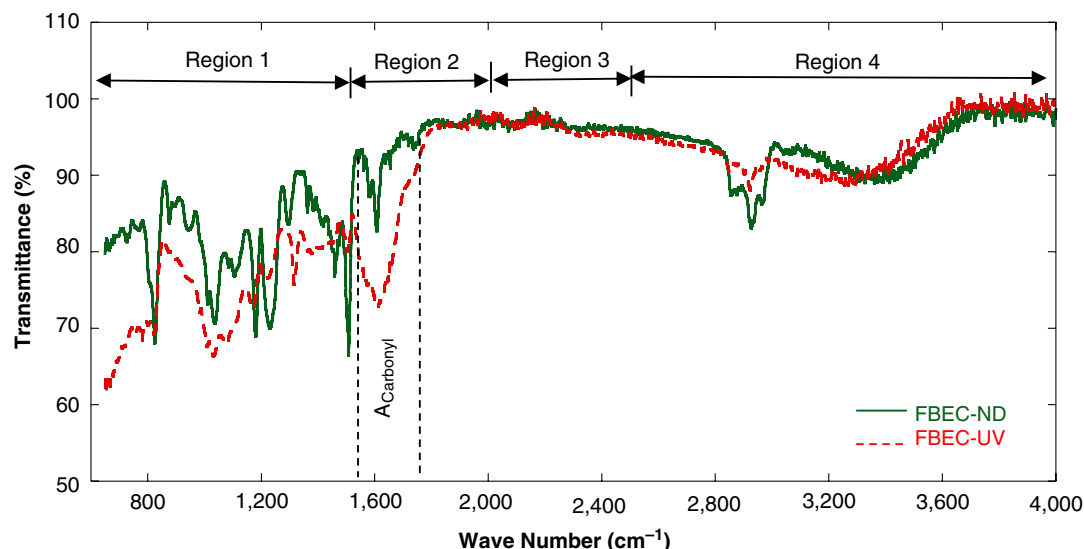


FIGURE 11. FTIR spectra of FBE coating with and without exposure to UV rays.

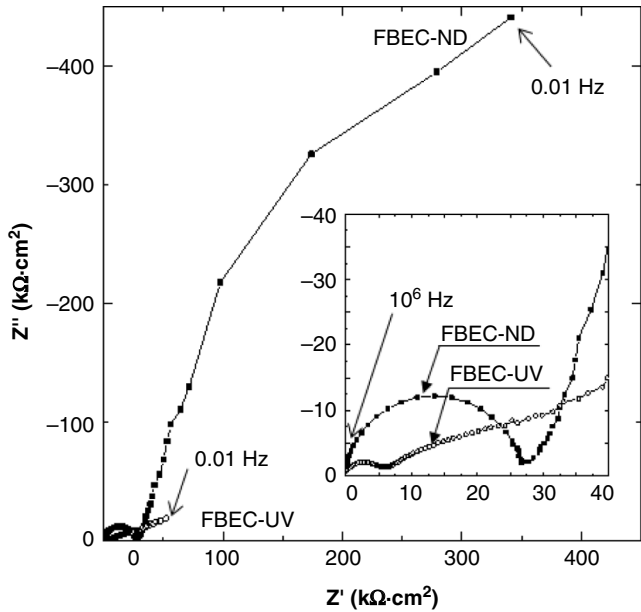


FIGURE 12. EIS response from FBE-coated steels—with and without UV exposure and then embedded in mortar.

allows the entry of more pore solution, moisture, and chlorides. The coating with interconnected pores/pinholes/cracks filled with moist corrosion products can exhibit a low coating resistance.

4.2.2 | FBEC-UV: Coating Degradation and Corrosion Initiation

Figure 13(b) shows the two-stage fast degradation process of FBEC-UV coating in cement mortar exposed to chlorides. The first five plots indicate the data collected from five specimens during the exposure of lollipop specimens with FBEC-UV steel rebars. The resistance of the coating was constant for about two cycles of exposure—indicating that the FBEC-UV coating could resist the penetration of moisture/chloride during this time. With further exposure, the resistance of FBEC-UV coating decreased significantly. The last drawing in Figure 13(b) shows the degradation process of FBEC-UV coating. Stage 1 is defined as the initial period when R_C offered by the coating was significantly high. Stage 2 is defined as the period when R_C decreases significantly. Unlike Stage 3 of FBEC-ND, the FBEC-UV specimens did not exhibit an increase in R_C . Stage 1 is defined as the initial period when R_C offered by the coating was significantly high. Stage 2 is defined as the period when

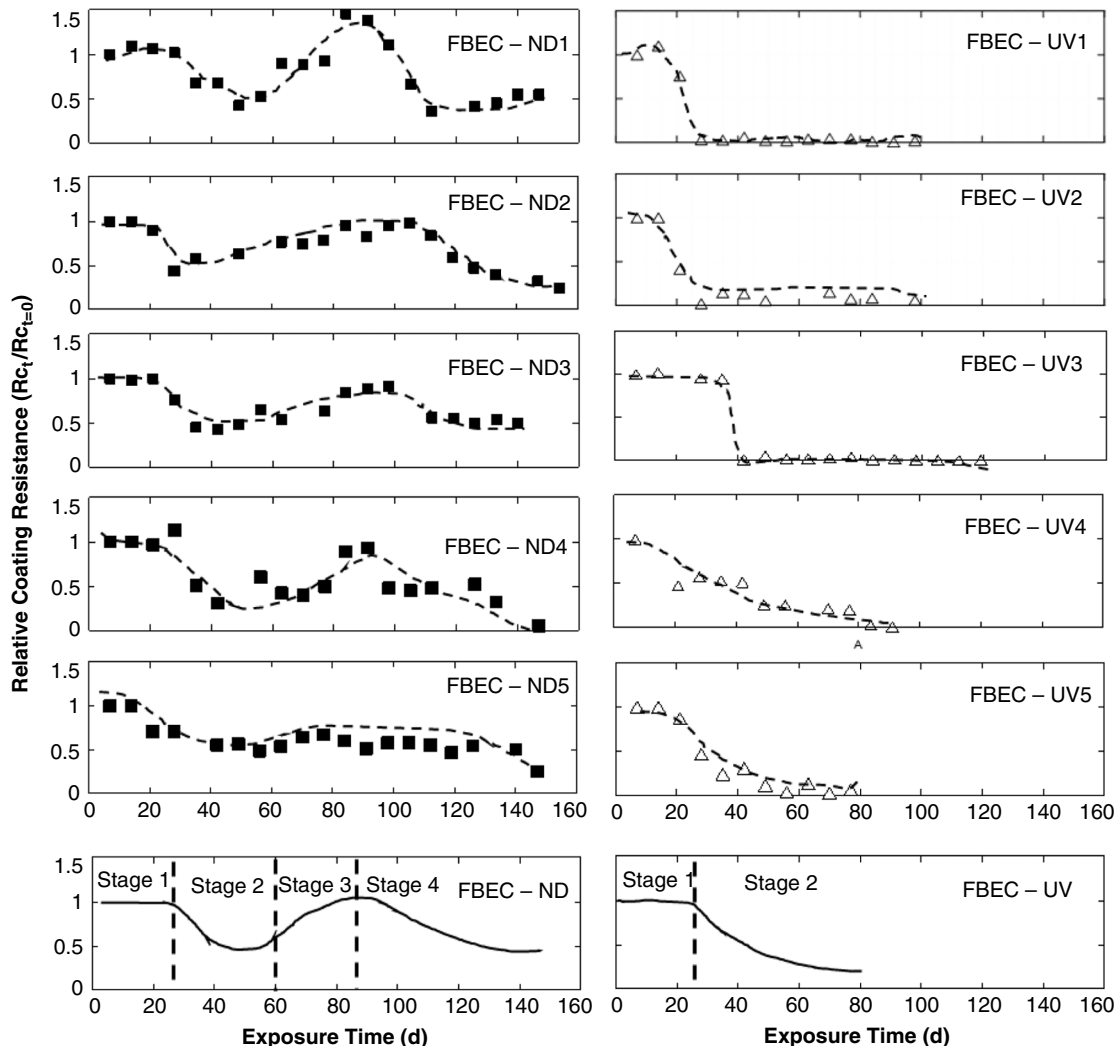


FIGURE 13. Change in relative resistance of coating due to exposure to cement mortar.

R_C decreases significantly. Unlike Stage 3 in the case of FBEC-ND, the FBEC-UV specimens did not exhibit an increase in R_C . The corrosion products formed in the case of FBEC-UV rebars can exert the expansive pressure and diffuse and permeate out through the cracks in the coating that can form within 10 d of exposure in UV chamber (see Figure 8). With further exposure, R_C continued to decrease, mainly because of the presence of chlorides and the formation of soluble corrosion products filling the space available in the coating.

Figure 14(a) shows the proposed mechanisms for the initiation of corrosion in concrete with FBE-coated steel rebars exposed to sunlight/UV rays. Note that all of the cracks are not the same depth. As shown, the metal surface below one of the deep cracks can act as an anode and another crack with moisture can provide a least resistive path (for ionic conduction) and the steel surface below can act as cathode.

The micrograph in Figure 14(b) shows such cracks formed in FBE coating. Also, such cracks can facilitate the transport of oxygen, moisture, and chlorides to the steel surface. Figure 14(c) shows a schematic of the propagation of underfilm corrosion and associated mechanisms. In this case, if the bond between steel and coating cannot resist the expansive forces, coating disbondment will occur—resulting in further propagation of underfilm corrosion,⁷² which is evident from Figure 14(d). The micrograph reveals that the corrosion progresses under the coating and corrosion products first fill the pores in the inner layer of FBE coating. To confirm this, the lollipop test specimens were autopsied and the coating surface and the steel surface (after removing the mortar cover) were visually inspected. Figure 14(e) shows a photograph and schematic of corroded FBEC-UV steel rebar with localized corrosion spots and underfilm corrosion. Therefore, for the structures that are already built

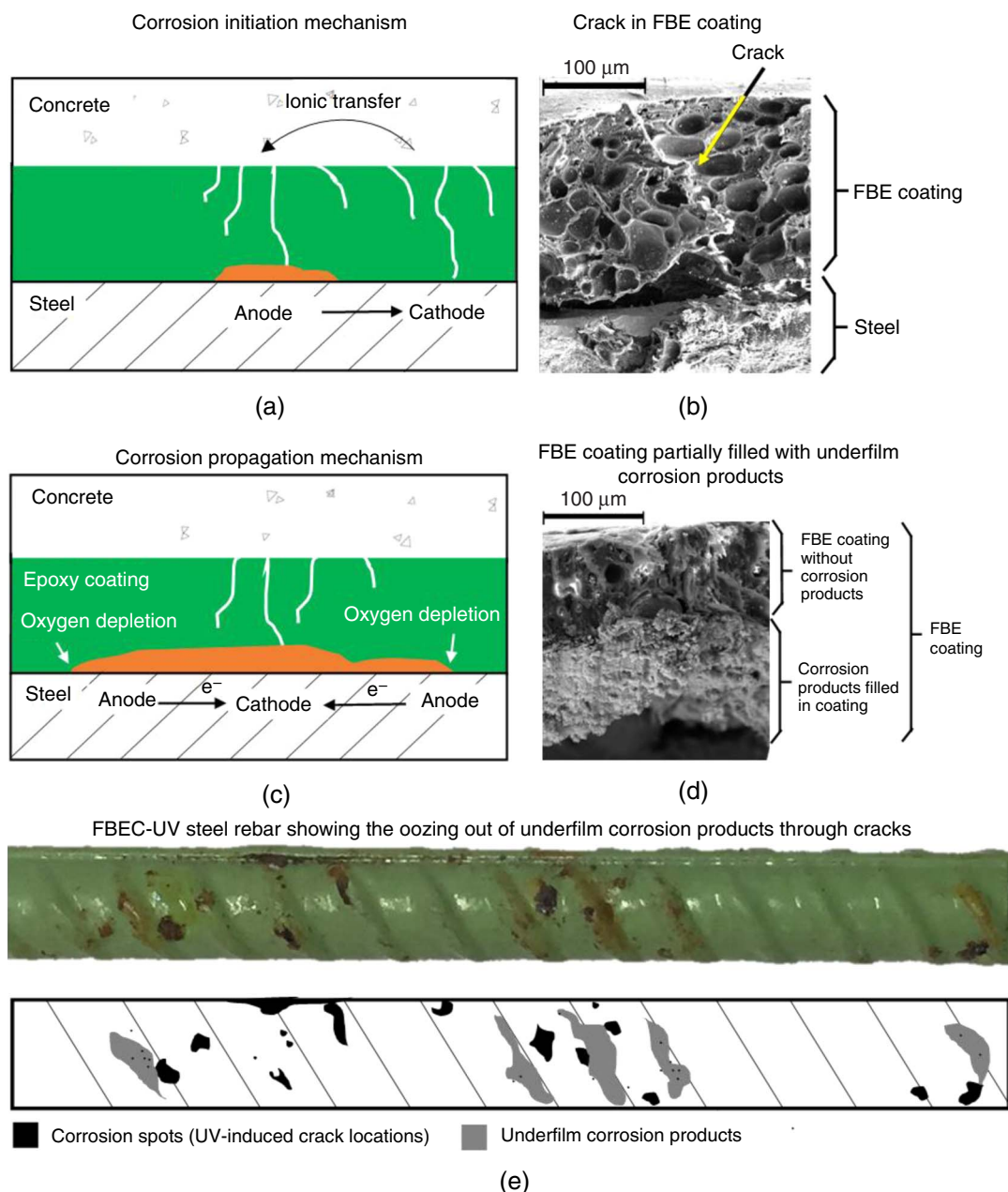


FIGURE 14. Proposed corrosion mechanisms of FBE-coated steel exposed to UV/sunlight and then embedded in concrete.

with FBE-coated steel rebars, it is essential to form preventive maintenance strategies to delay the initiation of corrosion in RC systems. For future construction, it is essential to prevent FBE-coated steel rebars from getting exposed sunlight/UV rays before placing them in concrete systems so that the coating can work effectively in resisting chloride attack.

4.2.3 | Determination of Chloride Threshold of Steel (Uncoated, ND, and UV)

The comparison of the polarization resistance of the steel or steel/coating interface (R_p or $R_{p,S-C}$) can be used as a short-term test for screening the steel rebars. However, evaluation based on chloride threshold (Cl_{th}) is a more rational approach to define the corrosion performance and service life of coated or uncoated steel rebars in cementitious systems. Figure 15(a) shows the variation of inverse polarization resistance (i.e., $1/R_p$) for uncoated rebars as a function of exposure time. Figures 15(b) and (c) show the variation of inverse polarization resistance (i.e., $1/R_{p,S-C}$) for FBE-coated rebars without and with UV exposure. The filled markers represent the points of active corrosion (i.e., after the initiation of corrosion). The specimens with uncoated steel rebars exhibited initiation of corrosion at about 50 d of cyclic wet-dry exposure to SPS solution with chlorides, whereas FBEC-ND and FBEC-UV specimens exhibited initiation of corrosion between 150 d and 170 d and between 50 d and 80 d of cyclic wet-dry exposure, respectively. The delay in the initiation of corrosion in FBEC-ND specimens can be attributed to its low chloride diffusion coefficient. On the other hand, the early initiation of corrosion in FBEC-UV specimens can be attributed to the easy ingress of chlorides through the cracked coating.

See Figure 16 for the mean and coefficient of variation of Cl_{th} observed for uncoated, FBEC-ND, and FBEC-UV specimens. The chloride threshold (Cl_{th}) of uncoated steel was found to be 0.42%bwob with a coefficient of variation of 0.1. The average

chloride concentrations on the coating surface (at the coating/mortar interface) were found to be 0.75%bwob and 0.53%bwob, which is in agreement with the chloride thresholds reported by Kahhaleh, et al.⁵⁰ However, these chlorides at the mortar/coating interface do not participate in the corrosion process at the steel/coating interface. Therefore, chlorides at the innermost layer of FBE coating (at the steel/coating interface) were determined and defined as Cl_{th} . In this manner, the average Cl_{th} for the FBEC-ND and FBEC-UV steel rebars were found to be 0.12%bwob and 0.07%bwob, respectively. This is about 1/4th of the Cl_{th} of uncoated steels. This significant difference in Cl_{th} of uncoated and coated steel rebars can be attributed to the differences in the pH of mortar (i.e., 12 ± 1) and of FBE coating (i.e., 6 ± 1) in contact with uncoated and coated steel rebars, respectively.⁷³⁻⁷⁴ Also, the difference in the size of cracks in coatings can lead to differences in the microclimate at the steel/coating interface (i.e., the concentration of oxygen and moisture), which in turn can lead to the difference in Cl_{th} between the uncoated, FBEC-ND, and FBEC-UV cases.

4.2.4 | Determination of Chloride Diffusion Coefficient of Coating and Service Life

Figure 17 shows the chloride profiles for FBEC-ND and FBEC-UV coatings. Note that, in FBEC-ND coatings, the chloride concentration at the first few micrometers away from the surface was significantly lower than that at the surface. This can be attributed to the closely packed microstructure of the FBEC-ND coating surface.⁷⁵ For the remaining depth, the chloride concentration was similar. In the case of FBEC-UV coatings, the chloride concentrations were found to be gradually decreasing as a function of the distance from the exposed coating surface (until the steel/coating interface). This can be attributed to the microcracking of FBE coating due to exposure to UV radiations and corresponding faster ingress of

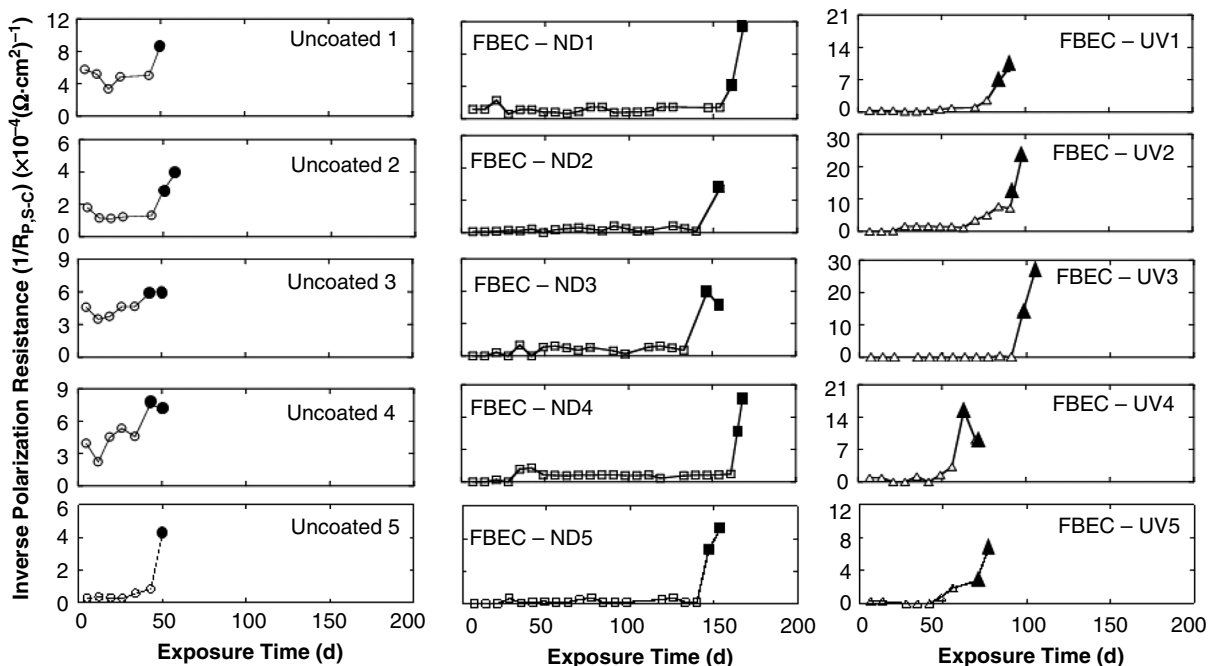


FIGURE 15. Detection of initiation of corrosion in lollipop specimens using EIS technique (unfilled and filled markers indicate passive and active corrosion measurements, respectively).

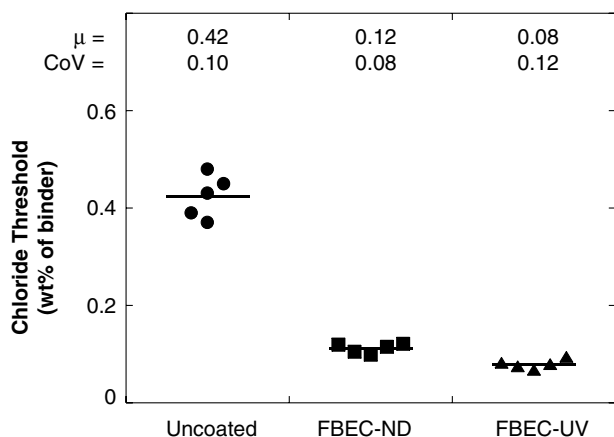
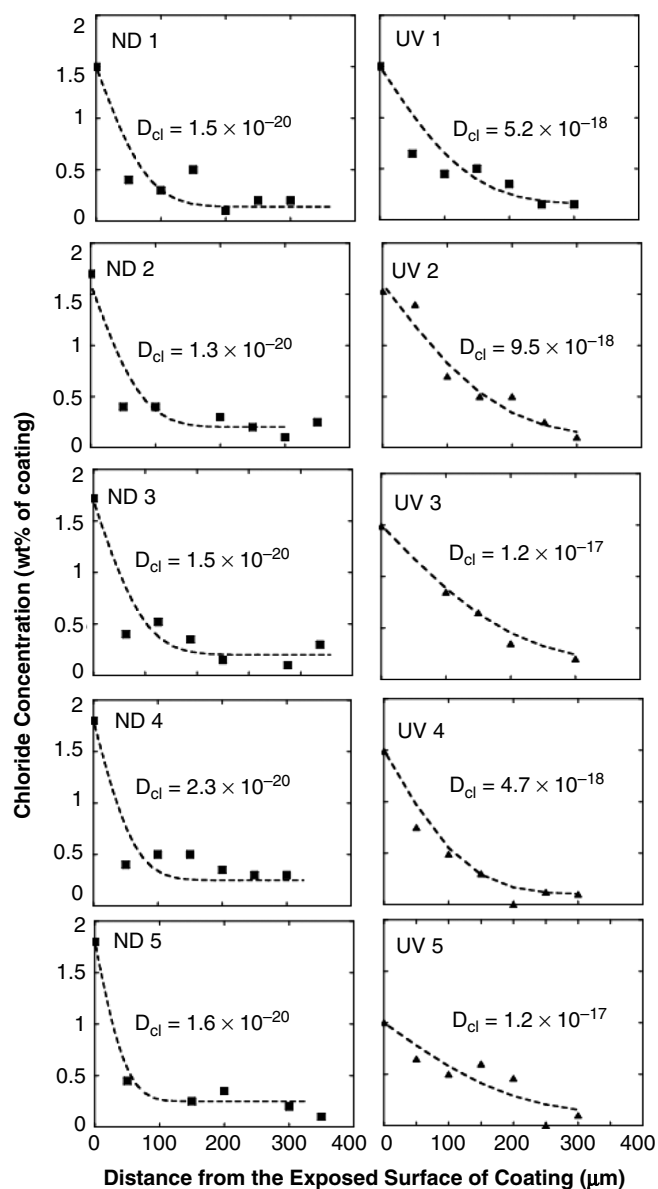


FIGURE 16. Chloride thresholds of uncoated and coated steels.



Note: All $D_{cl,coating}$ are presented in m^2/s

FIGURE 17. Chloride profile in coating at the time of corrosion initiation (obtained using EDX technique).

chlorides. The average $D_{cl,coating}$ for FBEC-ND and FBEC-UV coating specimens were found to be $1.6 \times 10^{-20} m^2/s$ and $8.7 \times 10^{-18} m^2/s$, with a coefficient of variation of 0.2 and 0.36, respectively. This significant difference between D_{cl} of ND and UV coatings indicates that the exposure to UV rays can severely degrade the coating—leading to faster ingress of chlorides. The $D_{cl,coating}$ in this study was found to be on the order of $10^{-18} m^2/s$ to $10^{-20} m^2/s$, which is in agreement with the results reported by Singh and Ghosh.⁵ On the other hand, for concrete, literature has reported the D_{cl} is more than $10^{-12} m^2/s$.⁷⁶

As a case study, the determined $D_{cl,coating}$ and Cl_{th} values were used to estimate the service life of a typical reinforced concrete systems with FBE-coated steel rebars. Figure 18 shows the cumulative distribution functions for the time to initiation of corrosion (traditionally defined as service life [t_i]) of reinforced concrete systems with uncoated, FBEC-ND, and FBEC-UV steel rebars. The input parameters used to obtain the cumulative distribution function are presented along with the cumulative distribution function. This case study shows that allowing FBE-coated rebars to get exposed to sunlight/UV for about 1 month can reduce the average expected service life from about 140 y to 45 y (reduction by about 70%). Also, the average t_i of element with FBEC-UV steel rebars was found to be about 30% less than that with the systems with uncoated steel rebars. Note that the results presented in this paper are for FBE-coated steel rebars exposed to UV rays for about 1 month. More than 1 month of exposure to sunlight can result in higher D_{cl} of FBE coating and lower t_i than what is presented in Figure 18. Also, the service life estimations presented here do not include all types of damages to epoxy-coated reinforcement. Thus, the real corrosion-free service life could be significantly less than what is presented here. Therefore, the use of FBE-coated steel is not beneficial if exposure to sunlight/UV cannot be avoided during various stages of transportation storage and construction.

$D_{cl,concrete}$	=	LN (1.7, 0.35) $\times 10^{-11} m^2/s$
C_{max}	=	LN (1.2, 0.03) %bwob
x	=	LN (50, 0.2) mm
m	=	0.3
$D_{cl,FBEC-ND}$	=	LN (1.6, 0.20) $\times 10^{-20} m^2/s$
$D_{cl,FBEC-UV}$	=	LN (8.6, 0.36) $\times 10^{-18} m^2/s$
Coating thickness	=	200 μm

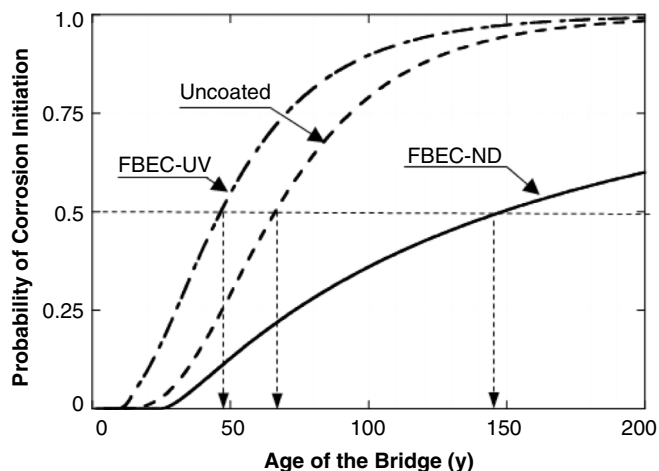


FIGURE 18. Cumulative distribution function for time to corrosion initiation.

RECOMMENDATIONS

Based on the results from microanalytical tests (SEM, EDX, and FTIR) on 45 coating samples and electrochemical tests on 15 uncoated and FBE-coated steel rebars, it is recommended to check the changes in the characteristics of epoxy coating and the chloride threshold of FBE-coated steels. The tests must be performed on coated steel samples that have been exposed to UV rays in the laboratory for 10 d or equivalent exposure time to represent the typical field exposure to sunlight/UV rays, and compared with the performance of uncoated steels. In addition to the coating requirements prescribed in ASTM A775, the following prescriptive and performance specifications are recommended:

- Number of cracks = zero: no cracks should appear on micrographs obtained at the magnification of 20,000
- Concentration of Ti on the coating surface >5 wt% of the coating
- Concentration of Zn on the coating surface >2 wt% of the coating
- Chloride diffusion coefficient of FBEC-UV coating should not be more than 1.2 times that of the chloride diffusion coefficient of FBEC-ND coating
- Average Cl_{th} (FBEC-ND) \approx average Cl_{th} (FBEC-UV)
- Service life concrete systems with FBE-coated steel rebars must be assessed using both the chloride threshold and chloride diffusion coefficients of concrete cover and FBE coating and must be greater than the desired service life
- Change the clause, "... to less than two months" in ASTM 775 (2017) to "FBE-coated steel rebars must be covered with opaque polyethylene sheeting to protect it from sunlight, salt spray, and weather exposure to minimize the total duration of sunlight/UV exposure to less than a month. The total duration of exposure includes the time during transportation, storage, and various construction stages until the coated steel rebars are embedded in concrete."

SUMMARY AND CONCLUSIONS

> Prolonged exposure of fusion-bonded epoxy (FBE) coated steel rebars to sunlight/ultraviolet (UV) rays during storage and staged/delayed construction is very common in civil construction sites. A comprehensive laboratory study was conducted to quantify the effect of exposure of FBE-coated steel rebars to UV rays on the coating characteristics, corrosion initiation characteristics, and the service life of concrete systems. Microanalytical results (FTIR/XRD/SEM/EIS) showed that about 1 month of UV exposure can result in shrinkage-induced cracking of coating due to the formation of carbonyl groups, preferentially at the locations with a deficiency of photostabilizers (TiO_2 and ZnO). Electrochemical results on steel-mortar lollipop specimens showed that the FBE coating without any damage/degradation (FBEC-ND) undergoes a four-stage slow degradation when exposed to alkaline and chloride environment, whereas UV-exposed FBE coating (FBEC-UV) undergoes a rapid two-stage degradation when exposed to cement mortar and chlorides. Mechanisms of degradation of epoxy coatings and the initiation of corrosion of FBE-coated steel rebars exposed to UV and then embedded in concrete are proposed. Based on cyclic wet-dry exposure of steel-mortar lollipop specimens, repeated EIS measurements, statistical analysis of inverse polarization resistance, and chemical and/or EDX tests, the chloride thresholds

for uncoated, FBEC-ND, and FBEC-UV steel rebars were determined to be 0.42%bwob, 0.12%bwob, and 0.07%bwob, respectively. It can be concluded that the chloride threshold (Cl_{th}) of FBE-coated steels is about 1/4th the chloride threshold of uncoated steels. Also, the chloride diffusion coefficient of coating ($D_{cl,coating}$) can increase by about two orders of magnitude (say, from 10^{-20} m²/s to 10^{-18} m²/s) when exposed to sunlight/UV rays. Based on the observed data on Cl_{th} and $D_{cl,coating}$, it is concluded that the exposure of FBE-coated steel rebars to sunlight/UV can decrease the service lives by about 70%, which in turn could be even 30% less than the service lives of systems with uncoated steel rebars. This paper also provides additional prescriptive/performance specifications for field practices to enhance and ensure long term corrosion resistance and durability of concrete structures.

ACKNOWLEDGMENTS

The authors acknowledge the financial support (Project No. EMR/2016/003196) received from the Science and Engineering Research Board, Department of Science and Technology and the partial financial support from the MHRD (Ministry of Human Resource Development) of the Government of India. The authors also acknowledge assistance from the faculty, laboratory staff, and students in the Construction Materials Research Laboratory (CMRL) in the Department of Civil Engineering, scanning electron microscopy facility in the Department of Metallurgical and Materials Engineering, FTIR facility in Department of Chemical Engineering at the Indian Institute of Technology Madras (IIT Madras), Chennai, India.

References

1. B. Blaz, X.R. Nóvoa, C. Pérez, A. Pintos, *Prog. Org. Coat.* 124 (2018): p. 275-285.
2. E.V. Cortés, "Corrosion Performance of Epoxy-Coated Reinforcement in Aggressive Environments" (Ph.D. diss., University of Texas at Austin, 1998).
3. S. Kessler, M. Zintel, C. Gehlen, *Struct. Concrete* 16 (2015): p. 398-405.
4. W.A. Pyc, "Field Performance of Epoxy-Coated Reinforcing Steel in Virginia Bridge Decks" (Ph.D. diss., Virginia Polytechnic Institute and State University, 1998).
5. D.D.N. Singh, R. Ghosh, *Corrosion* 61 (2005): p. 815-829.
6. D.G. Manning, *Constr. Build. Mater.* 10 (1996): p. 349-365.
7. A. Griffith, H.M. Laylor, "Epoxy Coated Reinforcement Study," *Oregon Department of Transportation Research Group, State Research Project 527*, June 1999.
8. F. Pianca, H. Schell, G. Cautillo, *Int. J. Mater. Product Technol.* 23 (2005): p. 286-308.
9. D. McDonald, "Epoxy-Coated Reinforcing Steel Bars in Northern America," Epoxy Interest Group of CRSI, 2009, available at: www.researchgate.net/publication/257121418_epoxy-coated_reinforcing_steel_bars_in_northern_america (June 19, 2020).
10. L.S. Cividanes, E.A.N. Simonetti, M.B. Moraes, F.W. Fernandes, G.P. Thim, *Polym. Eng. Sci.* 54 (2014): p. 2461-2469.
11. A.A. Sagúés, K. Lau, R.G. Powers, R.J. Kessler, *Corrosion* 66, 6 (2010): p. 065001-01 to 1065001-13.
12. R. Bhattacharya, S. Pal, A. Bhoumick, P. Barman, *Int. J. Eng. Sci. Technol.* 4 (2012): p. 4577-4583.
13. C. Heberlein, E. Bournay, H. Forster, J. Bennett, J.A. Dearing, J.S. Curliin, E. Gonin, S. Lemmet, R. Shende, R. Bisset, E. Clark, A. Fenner, S. De Gobert, B. Natarajan, K.M. Sharma, M. Williams, "Vital Ozone Graphics 2.0 Climate Link," UNEP DTIE, RRID-Arendal, 2008, available at: <https://ozone.unep.org/sites/default/files/Vital-Ozone-Graphics-3.pdf> (April 2020).
14. S. Singh, N.K. Lodhi, A.K. Mishra, S. Jose, S.N. Kumar, R.K. Kotnala, *Atmos. Environ.* 188 (2018): p. 60-70.
15. ASTM A775, "Standard Specification for Epoxy-Coated Steel Reinforcing Bars" (West Conshohocken, PA: ASTM International, 2017).

16. S. Nikafshar, O. Zabihi, M. Ahmadi, A. Mirmohseni, M. Taseidifar, M. Naebe, *Materials* 10 (2017): p. 1-18.
17. N. Peddamallu, K. Sridharan, T. Nakayama, R. Sarathi, *Polym. Compos.* 40, 4 (2019): p. 1556-1563.
18. R.J. Morgan, J.E. O'Neal, D.L. Fanter, *J. Mater. Sci.* 15 (1980): p. 751-764.
19. K.C. Cheng, C.M. Lin, S.F. Wang, S.T. Lin, C.F. Yang, *Mater. Lett.* 61 (2007): p. 757-760.
20. V.O. Startsev, M.P. Lebedev, K.A. Khrulev, M.V. Molokov, A.S. Frolov, T.A. Nizina, *Polym. Test.* 65 (2018): p. 281-296.
21. A.M. Fadi, M.I. Abdou, S.A. Al-Elai, M.A. Hamza, S.A. Sadeek, *Prog. Org. Coat.* 136 (2019): p. 105263.
22. S.M.N. Cambier, "Atmospheric Corrosion of Coated Steel; Relationship Between Laboratory and Field Testing" (Ph.D. diss., The Ohio State University, 2014).
23. U.M. Angst, M.R. Geiker, A. Michel, C. Gehlen, H. Wong, O.B. Isgor, B. Elsener, C.M. Hansson, R. François, K. Hornbostel, R. Polder, M.C. Alonso, M. Sanchez, M.J. Correia, M. Criado, A. Sagüés, N. Buenfeld, *Mater. Struct.* 50, 143 (2017): p. 1-24.
24. N.P. Sharma, B.K. Bhattarai, B. Sapkota, B. Kjeldstad, *Atmos. Environ.* 60 (2012): p. 428-435.
25. I. Fountoulakis, C.S. Zerefos, A.F. Bais, J. Kapsomenakis, M.E. Koukoulis, N. Ohkawara, V. Fioletov, H. De Backer, K. Lakkala, T. Karppinen, A.R. Webb, *Comptes Rendus Geosci.* 350 (2018): p. 393-402.
26. B. Mahltig, H. Böttcher, K. Rauch, U. Dieckmann, R. Nitsche, T. Fritz, *Thin Solid Films* 485 (2005): p. 108-114.
27. A. Ghasemi-Kahrizangi, H. Shariatpanahi, J. Neshati, E. Akbarinezhad, *Appl. Surf. Sci.* 353 (2015): p. 530-539.
28. M. Liu, A.R. Horrocks, *Polym. Degrad. Stabil.* 75 (2002): p. 485-499.
29. A. Ghasemi-Kahrizangi, H. Shariatpanahi, J. Neshati, E. Akbarinezhad, *Appl. Surf. Sci.* 331 (2015): p. 115-126.
30. D. Löf, G. Hamieau, M. Zalich, P. Ducher, S. Kynde, S.R. Midtgaard, C.F. Parasida, L. Arleth, G.V. Jensen, *Prog. Org. Coat.* 142 (2020): p. 105590.
31. B. Mahltig, H. Böttcher, K. Rauch, U. Dieckmann, R. Nitsche, T. Fritz, *Thin Solid Films* 485 (2005): p. 108-114.
32. B. Liu, Z.G. Fang, H. Bin Wang, T. Wang, *Prog. Org. Coat.* 76 (2013): p. 1814-1818.
33. X.H. Wang, Y. Gao, *Construct. Build. Mater.* 119 (2016): p. 185-205.
34. K.B. Tator, "Coating Deterioration," in *Protective Organic Coatings*, ed. K.B. Tator, *ASM Handbook* 5B (Materials Park, OH: ASM, 2015), p. 462-473.
35. A.A. Sagüés R.G. Powers, "Effect of Concrete Environment on the Corrosion Performance of Epoxy-Coated Reinforcing Steel," *CORROSION* 1990 (Houston, TX: NACE International, 1990).
36. A. Cao-Paz, A. Covelo, J. Farina, X.R. Nóvoa, C. Pérez, L. Rodríguez-Pardo, *Prog. Org. Coat.* 69 (2010): p. 150-157.
37. A. Miszczyk, K. Darowicki, *Prog. Org. Coat.* 124 (2018): p. 296-302.
38. F. Tang, G. Chen, R.K. Brow, M.L. Koenigstein, "Electrochemical Characteristics and Equivalent Circuit Representation of Mortar-Coating-Steel Systems by EIS," *CORROSION* 2014, paper no. 4090 (Houston, TX: NACE, 2014), p. 1-10.
39. K. Lau, A.A. Sagüés, *ECS Trans.* 13 (2007): p. 81-92.
40. L. Xing, D. Darwin, J. Browning, "Evaluation of Multiple Corrosion Protection Systems and Corrosion Inhibitors for Reinforced Concrete Bridge Decks," Federal Highway Administration & Kansas Department of Transportation, SM Report no. 99, 2010.
41. A.A. Sagüés, *Corrosion* 44 (1988): p. 555-557.
42. D. Darwin, M. O'Reilly, J. Browning, C.E. Locke, Y.P. Virmani, J. Ji, L. Gong, G. Guo, J. Draper, L. Xing, *J. Mater. Civil Eng.* 26 (2014): p. 1-9.
43. S. Rengaraju, "Electrochemical Response and Chloride Threshold of Steel in Highly Resistive Concrete Systems" (Ph.D. diss., Indian Institute of Technology Madras, 2019).
44. S. Kessler, U. Angst, M. Zintel, B. Elsener, C. Gehlen, *Mater. Corros.* 67 (2016): p. 631-638.
45. W.A. Pyć, R.E. Weyers, M. Weyers, D.W. Mokarem, J. Zemajtis, "Field Performance of Epoxy-Coated Reinforcing Steel in Virginia Bridge Decks," Virginia Department of Transportation, VTRC 00-R16, 2000.
46. G.R. Kim, S.H. Lee, H.Y. Song, J.M. Han, "Electrochemical Characterization of Epoxy Coated Steel Under Cathodic Protection," *CORROSION* 2007, paper no. 07013 (Houston, TX: NACE, 2007), p. 1-13.
47. F. Fanous, H. Wu, *J. Bridge Eng.* 10 (2005): p. 255-261.
48. J. Zemajtis, R.E. Weyers, M.M. Sprinkel, "Epoxy-Coated Reinforcement: A Historical Performance Review," *Virginia Transportation Research Council*, VTRC 97-IR1, 1996, p. 104.
49. R.N. Swamy, S. Koyama, *Construct. Build. Mater.* 3 (1989): p. 86-91.
50. K.Z. Kahhaleh, E. Vaca-cortés, J.O. Jirsa, H.G. Wheat, R.L. Carrasquillo, "Corrosion Performance of Epoxy-Coated Reinforcement-Macrocell Tests," Texas Department of Transportation, Research Project no. 1265-3, 1998.
51. M.S.H.S. Mohammed, R.S. Raghavan, G.M.S. Knight, V. Murugesan, *Arab J. Sci. Eng.* 39 (2014): p. 3535-3543.
52. O.S.B. Al-Amoudi, M. Maslehuddin, M. Ibrahim, *ACI Mater. J.* 101 (2004): p. 303-309.
53. W.T. Scannell, K.C. Clear, "Long-Term Outdoor Exposure Evaluation of Concrete Slabs Containing Epoxy-Coated Reinforcing Steel," Transportation Research Record, Concrete Reinforcing Steel Institute, 1990, p. 70-78.
54. A.B. Darwin, J.D. Scantlebury, *Cement Concrete Comp.* 24 (2002): p. 73-78.
55. L.W. McKeen, *Measurement of Coating Properties and Performance, Fluorinated Coatings Finishes Handbook*, 2nd ed. (Norwich, NY: William Andrew Publishing, 2006), p. 175-196.
56. ASTM G154-16 "Standard Practice for Operating Fluorescent Ultraviolet (UV) Lamp Apparatus for Exposure of Nonmetallic Materials" (West Conshohocken, PA: ASTM International, 2016).
57. R. Asmatulu, G.A. Mahmud, C. Hille, H.E. Misak, *Prog. Org. Coat.* 72 (2011): p. 553-561.
58. "Long-Term Weather Forecast Chennai, India," Weather Atlas, 2020, <https://www.weather-ind.com/en/india/chennai-long-term-weather-forecast> (April 17, 2020).
59. "ASTM G154 and G155 Explained," Element, 2016, <https://www.element.com/nucleus/2016/09/14/astm-g154-and-g155-explained> (June 16, 2020).
60. S. Rengaraju, L. Neelakantan, R.G. Pillai, *Electrochim. Acta* 308 (2019): p. 131-141.
61. D. Kamde, "Electrochemical, Bond, and Service Life Parameters of Coated Steel - Cementitious Systems Exposed to Chlorides" (Ph.D. diss. submitted for evaluation, Indian Institute of Technology Madras, 2020).
62. X.H. Wang, B. Chen, Y. Gao, J. Wang, L. Gao, *Construct. Build. Mater.* 93 (2015): p. 746-765.
63. J. Karuppanasamy, R.G. Pillai, *Mater. Struct.* 50 (2017): p. 1-17.
64. P.D. Cady, E.J. Gannon, "Appendix F: Standard Test Method for Chloride Content in Concrete Using the Specific Ion Probe" in *Condition Evaluation of Concrete Bridges Relative to Reinforcement Corrosion, Volume 8: Procedure Manual*, SHRP-S-330 (Washington, D.C.: National Research Council, 1993), p. 83-106.
65. D. Trejo, *personal discussion with Prof. David Trejo*, Oregon State University, 2020.
66. D.K. Kamde, R.G. Pillai, "Comparison of Corrosion of Damaged Fusion-Bonded-Epoxy-Coated (FBEC) and Uncoated Steel Rebars," 71st RILEM Annual Week (Chennai, India: RILEM, 2017).
67. M.J. Baker, J. Trevisan, P. Bassan, R. Bhargava, H.J. Butler, K.M. Dorling, P.R. Fielden, S.W. Fogarty, N.J. Fullwood, K.A. Heys, C. Hughes, P. Lasch, P.L. Martin-Hirsch, B. Obinaju, G.D. Sockalingum, J. Sulé-Suso, R.J. Strong, M.J. Walsh, B.R. Wood, P. Gardner, F.L. Martin, *Natural Protocols* 9 (2015): p. 1771-1791.
68. A. Suliga, E.M. Jakubczyk, I. Hamerton, A. Viquerat, *Acta Astronaut.* 142 (2018): p. 103-111.
69. Z. Wang, F. Liu, J. Li, C. He, X. Peng, *Acta Phys. Polon. A* 132 (2017): p. 1523-1526.
70. R.S.C. Woo, Y. Chen, H. Zhu, J. Li, J. Kim, C.K.Y. Leung, *Compos. Sci. Technol.* 67 (2007): p. 3448-3456.
71. A.A. Sagüés, A.M. Zayed, *Corros. Sci.* 30 (1990): p. 1025-1044.
72. H. Wan, D. Song, X. Li, D. Zhang, J. Gao, C. Du, *Materials* 10 (2017): p. 1-15.
73. S. Mundra, M. Criado, S.A. Bernal, J.L. Provis, *Cement Concrete Res.* 100 (2017): p. 385-397.
74. A.A. Sagüés, H.M. Perez-Duran, R.G. Powers, *Corrosion* 47 (1991): p. 884-893.
75. A.A. Javidparvar, B. Ramezanzadeh, E. Ghasemi, *Prog. Org. Coat.* 90 (2016): p. 10-20.
76. R.G. Pillai, R. Gettu, M. Santhanam, S. Rengaraju, Y. Dhandapani, S. Rathnarajan, A. S. Basavaraj, *Cement Concrete Res.* 118 (2019): p. 111-119.

NOMENCLATURE

%bwob	wt% of binder
Cl_{th}	Critical chloride threshold of steel-coating or steel/mortar interface
C_{max}	Maximum chloride concentration at the exposed concrete surface
CPE	Constant phase element
CPE_C	Capacitance of the coating
CPE_M	Capacitance of the mortar
CPE_{S-C}	Capacitance of the steel/coating interface
D_{cl}	Chloride diffusion coefficient of concrete
$D_{cl,coating}$	Chloride diffusion coefficient of FBE coating
EIS	Electrochemical impedance spectroscopy
EEC	Equivalent electrical circuit
FBE	Fusion-bonded-epoxy
FBEC-ND	FBE-coated steel rebars in as-received condition with no damage/degradation
FBEC-UV	FBE-coated steel rebars after 10 days of UV exposure
m	Maturity coefficient
R_C	Resistance of the coating
$R_{p,S-C}$	Polarization resistance of the steel/coating interface
R_M	Resistance of the mortar
R_S	Resistance of electrolyte solution
S-C	Steel/Coating interface
t_i	Time to corrosion initiation
UV	Ultraviolet
x	Depth from the exposed surface of concrete
x_{epoxy}	Depth from the exposed surface of epoxy coating